# Irrigation quantification through backscatter data assimilation with a buddy check approach

**L. Busschaert[1], M. Bechtold[1], S. Modanesi[2], C. Massari[2], L. Brocca[2], G.J.M. De Lannoy[1]**

[1]Department of Earth and Environemental Sciences, KU Leuven, Heverlee, B-3001, Belgium
[2]Research Institute for Geo-hydrological Protection, National Research Council, Via della Madonna Alta 126, 06128 Perugia, Italy

**Key Points:**

- Model-driven irrigation estimation has limitations, when solely based on improved soil moisture conditions obtained via data assimilation.
- A new method based on an adaptive outlier detection improves the estimated irrigation in a synthetic data assimilation setup.
- The method reduces irrigation errors by 30% for frequent assimilation of backscatter observations with reasonable levels of noise.

Corresponding author: Louise Busschaert, `louise.busschaert@kuleuven.be`

## Abstract

Irrigation is an important component of the terrestrial water cycle, but it is often poorly accounted for in models. Recent studies have attempted to integrate satellite data and land surface models via data assimilation (DA) to (1) detect and quantify irrigation, and (2) better model the related land surface variables such as soil moisture, vegetation, and evapotranspiration.

In this study, different synthetic DA experiments are tested to advance satellite DA for the estimation of irrigation. We assimilate synthetic Sentinel-1 backscatter observations into the Noah-MP model coupled with an irrigation scheme. When updating soil moisture, we found that the DA sets better initial conditions to trigger irrigation in the model. However, large DA updates to wetter conditions can inhibit irrigation simulation. Building on this limitation, we propose an improved DA algorithm using a buddy check approach. The method still updates the land surface, but now the irrigation trigger is not based on the evolution of soil moisture, but on an adaptive innovation outlier detection.

The new method was tested with different levels of model and observation error. For mild model and observation errors, the DA outperforms the model-only 14-day irrigation estimates by about 30% in terms of root-mean-squared differences, when frequent (daily or every other day) observations are available. The improvements can surpass 50% for high forcing errors. However, with longer observation intervals (7 days), the system strongly underestimates the irrigation amounts. The method is flexible and can be expanded to other DA systems and to a real world case.



## Plain Language Summary

Irrigation has an important impact on the terrestrial water cycle. However, it remains poorly simulated by models and it is hard to quantify through satellite observations alone. The combination of both models and satellite observations to detect and quantify irrigation has been explored in the last few years. Recently, Sentinel-1 radar (microwave) observations have been assimilated into the Noah-MP land surface model in order to quantify irrigation, and better estimate the related land surface variables, such as soil moisture and vegetation. This system has shown benefits but also limitations, which are highlighted and addressed in our study using synthetic experiments. We proposed an improved data assimilation algorithm and tested it for different levels of model and observation error. The new method estimates irrigation more accurately (30%) than the model alone, provided that frequent (daily or every other day) observations are available. With further developments, the new methodology could be used in a real-world experiment where it could ultimately contribute to the complex challenge of irrigation monitoring.


## 1 Introduction

Irrigation represents more than 70% of freshwater withdrawals (Gleick et al., 2009) making it the most important human activity impacting the terrestrial water cycle. Over the last decades, irrigated areas have expanded almost sixfold (Siebert et al., 2015), and contributed significantly to the increase in global crop production over the same time period (Foley et al., 2011). Under a growing population, food demand will continue to rise, which will inevitably lead to a further expansion and intensification of irrigated agriculture (Foley et al., 2011). In parallel, climate change will impact the irrigation water needs as a result of the expected rising temperatures and drier periods in many regions (Busschaert et al., 2022; Döll, 2002; Fischer et al., 2007). Conversely, irrigation also plays an important role in weather and climate dynamics (Bonfils & Lobell, 2007; Hirsch et al., 2017; Mahmood et al., 2014; Thiery et al., 2017, 2020), but it is still not or poorly included in Earth system models (Cook et al., 2015; Gormley-Gallagher et al., 2022; Valmassoi & Keller, 2022). Not only is there a call to monitor irrigation in order to ensure that the available water meets the

future irrigation demands, but future climate-related research, and Earth system models in general, could significantly benefit from large-scale irrigation estimates.

In the last years, several methods have been developed to map and quantify irrigation by making use of satellite remote sensing data (Massari et al., 2021). These observations (optical, microwave and gravimetric measurements) are used alone, combined with each other, or with models. Optical observations were first used to map irrigation relying on the difference in spectral responses between irrigated and non-irrigated areas (e.g., Ozdogan & Gutman, 2008; Pervez et al., 2014; Salmon et al., 2015; Xie & Lark, 2021; L. Zhang et al., 2022), and more recently machine learning-based methods have also been suggested (e.g., Jin et al., 2016; Magidi et al., 2021; Nagaraj et al., 2021; C. Zhang et al., 2022). Optical data have further been used to quantify irrigation amounts, mostly using estimates of actual evapotranspiration (ET) based on vegetation indices, sometimes also including models (land surface, water and energy balance), or other remote sensing data (e.g., thermal) (e.g., Brombacher et al., 2022; Bretreger et al., 2022; Droogers et al., 2010; Le Page et al., 2012; Maselli et al., 2020; Olivera-Guerra et al., 2020; van Eekelen et al., 2015; Vogels et al., 2020). More recently optical leaf area index (LAI) observations have been assimilated into the Noah-MP land surface model (LSM; Niu et al., 2011) with a focus on improving irrigation estimations by updating the land surface (Nie et al., 2022).

While optical-based methods have progressed and shown some promising results, they typically rely on proxies, and are limited by cloud cover. By contrast, microwave signals can directly be related to water, and are not limited by atmospheric conditions. Despite their coarse resolutions, soil moisture retrievals from passive L-band radiometers or from active C-band scatterometers can detect wetter moisture when large-scale irrigation water is applied. The first microwave-based irrigation estimates were derived by inverting the soil water balance (SM2RAIN algorithm; Brocca et al., 2014) using several surface soil moisture (SSM) products (Soil Moisture Active Passive [SMAP], Soil Moisture Ocean Salinity [SMOS], Advanced SCATterometer [ASCAT], Advanced Microwave Scanning Radiometer 2 [AMSR2]) at a 25-km resolution (Brocca et al., 2018). They found satisfactory results in terms of irrigation quantification, but the outcome strongly depended on the revisit and the uncertainty of the SSM retrievals. Following the same approach, Dari et al. (2020) achieved finer resolution quantification by downscaling SMAP and SMOS data using the Disaggregation based on Physical and Theoretical scale Change algorithm (DisPATCh; Merlin et al., 2008). Jalilvand et al. (2019) applied this method in a more arid climate (Iran). SSM retrievals (containing irrigation in the signal) were also contrasted against LSM simulations (without irrigation), in order to estimate the amounts of water applied (Zaussinger et al., 2019; Zohaib & Choi, 2020). Despite these methodological advances towards irrigation estimation, the currently most accurate microwave-based satellite SSM retrievals are, for the time being, only available at resolutions coarser than most irrigated fields in Europe.

C-band synthetic aperture radar (CSAR) observations provide data at finer (field scale) resolutions, and they are also sensitive to soil moisture, albeit with less penetration depth than L-band observations. The Sentinel-1 (S1; Torres et al., 2012) mission from the European Space Agency (ESA) offers the opportunity for frequent (∼2-3 day revisit in Europe) and fine-scale (10 m) observations, which are required for irrigation detection and quantification purposes. The S1 mission comprises a constellation of two satellites (S1-A and S1-B) sensing in two polarizations over land: co-polarized VV (vertically transmitted, vertically received), and cross-polarized VH (vertically transmitted, horizontally received). In December 2021, S1-B has become unresponsive, resulting in fewer observations from that time onwards. High-resolution SSM estimates retrieved from S1 backscatter have been developed in the last years. Zappa et al. (2021) used the TU Wien S1 SSM product (Bauer-Marschallinger et al., 2019) to detect and quantify irrigation at a local scale, based on spatiotemporal variations in SSM. The method showed promising results in terms of detection and correlation, but systematic underestimations of the irrigation water amounts were found when the observation interval was longer than 1 day (in a follow-up synthetic experiment; Zappa et al., 2022). The

first regional datasets of high resolution irrigation water use, based on S1 data, have been released by (Dari et al., in review) using the soil moisture-based inversion approach. While the backscatter itself has already been used in irrigation mapping and timing studies at the local scale (Bazzi, Baghdadi, Fayad, Zribi, et al., 2020; Bazzi, Baghdadi, Fayad, Charron, et al., 2020), the direct use of S1 data to quantify irrigation is only in its infancy, as changes in backscatter are affected by the water in the topsoil, but also by the vegetation (water, volume, density, and geometry), and terrain roughness (McNairn & Shang, 2016).

The most optimal and spatio-temporally complete estimates of irrigation could theoretically be expected to result from a combination of observations (e.g. microwave observations) with models through data assimilation (DA; De Lannoy et al., 2022). Abolafia-Rosenzweig et al. (2019) performed SMAP SSM DA into the variable infiltration capacity (VIC) LSM, using a particle batch smoother. With the intent of going to a finer resolution, Das et al. (in review) used a similar approach using the S1-SMAP SSM product (Das et al., 2019). Ouaadi et al. (2021) assimilated S1-derived SSM data into the FAO-56 (Allen et al., 1998) model with a particle filter. In the three aforementioned studies, a series of DA synthetic experiments were carried out to evaluate the impact of e.g., time interval between the assimilated observations and their level of error. They concluded that the proposed techniques could accurately estimate irrigation amounts and timing (only for Ouaadi et al., 2021) but that small errors (levels of noise) and frequent observations are crucial.

The above studies assimilated SSM products, but retrievals can introduce errors and inconsistencies in the DA system (De Lannoy et al., 2022). Indeed, microwave-based retrievals often rely on ancillary data, and on empirical change detection algorithms in the case of active measurements. Moreover, retrievals typically need rescaling to remove the bias between the forecast (modeled) and observed soil moisture to achieve an optimal DA system. These rescaling approaches sometimes remove irrigation from the signal (Kwon et al., 2022). Based on these limitations, Modanesi et al. (2022) decided to directly assimilate the S1 backscatter signal into the Noah-MP LSM (Niu et al., 2011) equipped with a sprinkler irrigation scheme (Ozdogan et al., 2010), where irrigation is dynamically modeled and triggered based on a soil moisture deficit approach. The DA updated SSM and LAI using an Ensemble Kalman Filter (EnKF) and a calibrated Water Cloud Model (WCM; Attema & Ulaby, 1978; Modanesi et al., 2021) as observation operator to map between SSM, LAI and backscatter. The idea is to provide the model with a better initial state, in terms of soil moisture and vegetation, to improve the triggering and estimation of irrigation. However, the method has also shown several limitations related to the model (soil texture, crop type, irrigation parametrization), and the DA system itself. An important problem is that irrigation events could be missed when the DA updates soil moisture to wetter conditions and thereby preventing irrigation simulation.

We set up synthetic experiments based on the system of Modanesi et al. (2022) with the goal to investigate the exact benefits and shortcomings of S1 backscatter DA and to improve the DA system with irrigation modeling (Section 2). In this context, synthetic backscatter observations are generated from a nature run (also called 'truth') with a calibrated WCM as observation operator (Modanesi et al., 2021). These observations are then assimilated into model simulations, for which the forcings are altered compared to the reference nature run. We then propose and test a novel method based on a buddy check approach. The land surface state is still updated to have better initial conditions to estimate irrigation, but the DA system now includes an adaptive innovation (observation *minus* forecast) outlier detection. Anomalous high backscatter observations are not assimilated but used to flag an unmodeled process and trigger irrigation when the conditions required for irrigation are met, i.e., dry soil moisture and growing season. This new method is evaluated for different forcing errors, observation intervals and observation errors in Section 3. Finally, we discuss (Section 4) the possible future developments of the method, along with the opportunity to bring this system to a real world experiment.

# 2 Data and Methods

## 2.1 Land surface model and irrigation scheme

This study is based on the system developed by Modanesi et al. (2022) in which the Noah-MP LSM version 3.6 (Niu et al., 2011), equipped with a sprinkler irrigation module (Ozdogan et al., 2010), is run within the NASA Land Information System (LIS) version 7.4 (Kumar et al., 2006, 2008). The LSM has four soil layers corresponding to the following depths: 0-10 cm (surface soil moisture; SSM), 10-40 cm (SM1), 40-100 cm (SM2), and 100-200 cm (SM3).

The irrigation scheme, coupled to the Noah-MP LSM, was initially developed by Ozdogan et al. (2010) and based on a soil moisture deficit approach. In the case of a fully irrigated pixel, the irrigation scheme depends on two conditions for irrigation to be triggered: (1) the day must fall within the growing season, and (2) the rootzone soil moisture must reach a certain depletion. First, the growing season is defined by a greenness vegetation fraction (GVF [-]) threshold, $GVF_{irr}$, as suggested by Ozdogan et al. (2010):

$$GVF_{irr} = GVF_{min} + 0.4 * (GVF_{max} - GVF_{min}) \tag{1}$$

In this study, GVF is based on a monthly climatology, and $GVF_{min}$ and $GVF_{max}$ are respectively the minimum and maximum monthly GVF. Second, the soil must be dry enough, meaning that the rootzone soil moisture has to reach a certain depletion. In the irrigation scheme, the depletion is defined by the moisture availability ($MA$ [-]) as follows:

$$MA = \frac{\sum_{l=1}^{lroot} \theta_l * RD_l - \sum_{l=1}^{lroot} \theta_{PWP} * RD_l}{\sum_{l=1}^{lroot} \theta_{FC} * RD_l - \sum_{l=1}^{lroot} \theta_{PWP} * RD_l} \tag{2}$$

where $\theta_l$ [-] and $RD_l$ [m] are the soil moisture content and rooting depth of the $l^{th}$ soil layer, and $\theta_{PWP}$ [-] and $\theta_{FC}$ [-] are the water contents at permanent wilting point and field capacity of the corresponding soil texture. The considered soil layers in the computation of $MA$ vary over the growing season given that $RD$ directly depends on the GVF, i.e.

$$RD = GVF * RD_{max} \tag{3}$$

in which $RD_{max}$ [m] is the maximum rooting depth (a vegetation parameter), and GVF is based on a monthly climatology (as in Equation 1). When both conditions (growing season and dry soil) are fulfilled, irrigation is triggered and the amount of water required brings the rootzone soil moisture back to field capacity. The irrigation rate ($Irr_{rate}$ [mm $s^{-1}$]) is then defined as follows:

$$Irr_{rate} = \frac{\sum_{l=1}^{lroot} (\theta_{FC} - \theta_l) * RD_l * 1000}{Irr_{time}} \tag{4}$$

where the $Irr_{time}$ (in seconds) corresponds to the period when irrigation is allowed. This time frame is set to 06:00 to 10:00 LT following Ozdogan et al. (2010). The $Irr_{rate}$ is then added to the precipitation at each model time step. In our study, we report the total irrigation amount per day, which is effectively applied at each model time step within the 4-hour irrigation period.

## 2.2 Nature run and synthetic observations

The Noah-MP with irrigation module was used to create a nature run (also called the *'truth'*) that provides reference data of soil moisture, LAI, and irrigation, along with all other variables. This output was also used to generate synthetic $\gamma^0_{VV}$ observations (via a calibrated WCM) that were assimilated in the different synthetic DA experiments.

The model was run at a temporal resolution of 15 min and at a 0.01° x 0.01° lat-lon spatial resolution, and the results are only shown for a single sandy loam pixel that is fully irrigated in Italy (44.565°N, 11.525°E). The scientific findings are the same for any pixel in this synthetic study, and our setup can be readily expanded to a large domain. Meteorological data to force the nature run were extracted from the Modern-Era Retrospective analysis for Research and Applications version 2 (MERRA2; Gelaro et al., 2017), which were remapped from a spatial resolution of 0.5° x 0.625° to the resolution of this study by bilinear interpolation. Soil texture parameters were taken from the 1 km Harmonized Soil World Database (HWSD v1.21). Irrigation was triggered when the $MA$ reached 0.45. This nature simulation ran over the period from 2010 through end 2019 after a model spin-up starting on 1 January 2000. Based on the GVF climatology (0.144° spatial resolution; Gutman & Ignatov, 1998) at this location, the growing season was defined as the months covering April through September.

Synthetic $\gamma^0_{VV}$ observations were generated daily (at 06:00 LT) from the nature run by propagating the SSM and LAI estimates through a calibrated WCM, which is considered to be perfect (*'true'*), just like the LSM, in this synthetic study. The WCM describes the soil and vegetation scattering processes through semi-empirical formulas (Attema & Ulaby, 1978) and therefore uses SSM and LAI from the LSM to simulate backscatter. The WCM calibration was based on input from a model simulation with irrigation simulation activated and real S1 backscatter observations, following Modanesi et al. (2021, 2022). The synthetic observations are assimilated after perturbing them with different levels of Gaussian white noise, with standard deviations ranging from 0 to 0.7 dB (see Section 2.3).

## 2.3 Experiments

### *2.3.1 Model-only run*

An overview of all experiments is given in Figure 1. Model-only runs, also called open-loop (OL), were performed with the same settings and inputs as the nature run, but with an introduction of forcing error. Specifically, the meteorological forcings were altered in two different ways: (1) all forcings were kept identical to the nature run (MERRA2) except for precipitation which was shifted in time (using 2000-2009, instead of 2010-2019), referred to as $\mathrm{OL}_H$ (high forcing error); and (2) all MERRA2 forcings were replaced with the European Center for Medium-Range Weather Forecasts (ECMWF) Reanalysis version 5 (ERA5; Hersbach et al., 2020), referred to as $\mathrm{OL}_M$ (mild forcing error). For the first case, shifting the MERRA2 precipitation (also performed by Girotto et al., 2021) introduces long-term errors since the interannual variability of the precipitation deviates from the truth. By contrast, the experiments with mild forcing errors will use monthly and annual precipitation patterns that are closer to the truth and the errors mostly represent short-term deviations. The OL experiments served as a reference to assess the skill gain of the DA experiments.

### *2.3.2 Default DA experiments*

In the default DA experiments ($\mathrm{DA}_1$), daily synthetic $\gamma^0_{VV}$, without any addition of noise, are assimilated to update the SSM at all update time steps. The irrigation scheme is primarily triggered by the (updated) soil moisture deficit, similar to the OL. In line with the OL simulations, the $\mathrm{DA}_1$ experiments were also run for a high ($\mathrm{DA}_{1,H}$) and mild ($\mathrm{DA}_{1,M}$) forcing error. The aim of $\mathrm{DA}_1$ is to identify the strengths and weaknesses of the approach by Modanesi et al. (2022).

### *2.3.3 Buddy check DA experiments*

The last series of experiments aim at testing the newly proposed buddy check approach ($\mathrm{DA}_2$) described in Section 2.4.2. Similar to above, the DA was tested for setups of forcing error, i.e. $\mathrm{DA}_{2,H}$ and $\mathrm{DA}_{2,M}$. The method was tested for daily perfect (no white noise)

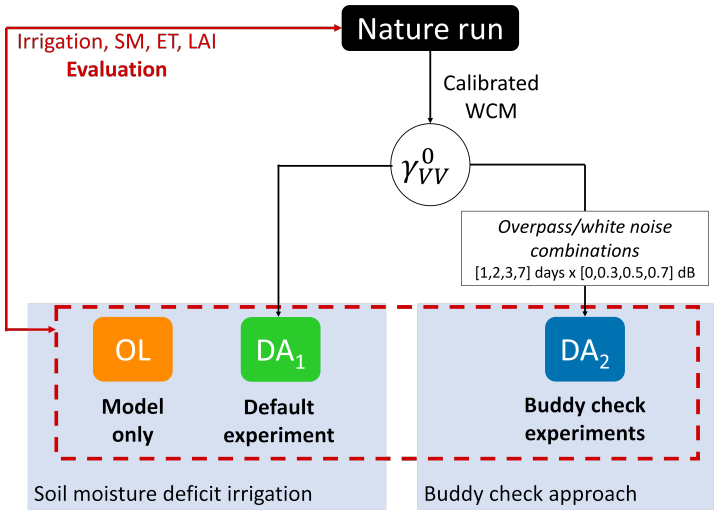


**Figure 1.** Overview of the experiments. Note that all experiments are repeated for high forcing error ($OL_H$, $DA_{1,H}$, $DA_{2,H}$) and mild forcing error ($OL_M$, $DA_{1,M}$, $DA_{2,M}$).

observations, as well as for different overpass intervals (one observation every 1, 2, 3, and 7 days), and different white noise levels in the assimilated observations. White noise is added to the observations in time through a Gaussian distribution of mean zero and different standard deviations ($\sigma$): 0, 0.3, 0.5, and 0.7 dB. This range in total observation error (measurement+representativeness error) was chosen considering the fact that the S1 CSAR instruments on board of S1-A and S1-B have respective radiometric accuracies ($1\sigma$) of 0.25 dB and 0.32 dB (varying with the acquisition mode and polarization; Miranda et al., 2017) and that the observation operator is assumed to be perfectly calibrated (i.e. the calibrated WCM is the truth), which limits the representativeness error (van Leeuwen, 2015). Note that when white noise was added to the signal, experiments were run for three different seeds of random noise.

#### *2.3.4 Ensembles*

For all experiments (OL, $DA_1$, and $DA_2$), a total of 24 ensemble members were used. The ensembles were generated by perturbing model forcings (rainfall, incident longwave radiation, incident shortwave radiation) and the SSM state variable (only, i.e. the uncertainty on LAI is assumed to be marginal). For further details on the perturbation parameters, the reader can refer to Modanesi et al. (2022). It should be noted that in contrast to the setup of Modanesi et al. (2022), a perturbation bias correction method was applied in this study. This adjustment was proposed by Ryu et al. (2009) to avoid unintended biases in the forecast of soil moisture. To be able to use this option with the soil moisture deficit irrigation approach (OL and $DA_1$), the conditions for which irrigation is triggered required slight modifications. In the Noah-MP v3.6 LSM, irrigation is triggered by looking at the $MA$ of each ensemble member individually. This is not compatible with the perturbation bias correction option as the correction can bring the soil moisture of several ensemble members sooner to an irrigation state when some other members have not reached the $MA$ threshold yet. Therefore, in this study and for all experiments, irrigation was triggered based on the ensemble mean $MA$ and the same amount of irrigation water (also calculated from the ensemble mean) is applied to each ensemble member. This was already corrected in the irrigation module of the latest Noah-MP version (4.0.1).

## 2.4 Data assimilation

### *2.4.1 State updating*

Synthetic observations of co-polarized backscatter ($\gamma^0_{VV}$) were assimilated to update the SSM, and all other variables via model propagation. An ensemble Kalman filter (EnKF) was employed to ingest $\gamma^0$ observations into an erroneous version of the Noah-MP LSM (i.e. different from that of the nature run, see Section 2.3). The 24 ensemble members were used to derive the forecast error. The *'true'* calibrated WCM was used as observation operator to produce observation predictions based on the erroneous LSM simulations of SSM and LAI. The update equation of the EnKF can be written as follows:

$$\widehat{x_i^+} = \widehat{x_i^-} + K_i[y_{obs,i} - h_i(\widehat{x_i^-})] \tag{5}$$

for which $\widehat{x_i^+}$ is an ensemble of the updated model states at time step $i$, $\widehat{x_i^-}$ is the ensemble forecast state, $y_{obs,i}$ is the assimilated observation ($\gamma^0_{VV}$), $K_i$ is the Kalman gain, and $h_i(.)$ is the WCM observation operator. The innovation at time $i$ ($innov_i$) is defined as the residual between the observed and the forecast $\gamma^0_{VV}$ and is expressed in decibels (dB):

$$innov_i = y_{obs,i} - h_i(\widehat{x_i^-}) \tag{6}$$

Even though the observation predictions use both SSM and LAI as input, the update is limited to SSM here for simplicity (unlike Modanesi et al., 2022).

### *2.4.2 Buddy check approach*

Because Modanesi et al. (2022) reported that DA updates to a wetter soil moisture could possibly lead to missed simulated irrigation events, we tested a novel approach in this study, illustrated in Figure 2 for a case with daily observations. We still update SSM as proposed above. However, the triggering of irrigation is now not merely based on a modeled soil moisture deficit, but instead always requires a high positive difference between the observed and forecast $\gamma^0_{VV}$ (innovation; Equation 6). In other words, the timing of the irrigation is now primarily observation-based. The new method builds on a simple buddy check approach, commonly used in atmospheric DA (e.g., Dee et al., 2001), avoiding the assimilation of outlier observations. In this case, outliers are detected when the innovation is suddenly large and positive, corresponding to a significantly higher observed than forecasted $\gamma^0_{VV}$ (highlighted blue dots in Figure 2a). This 'jump' in the innovations can be detected by looking at the difference between two successive innovations. This will be referred to as $\Delta innov_i$, defined as:

$$\Delta innov_i = innov_i - innov_{i-T} \tag{7}$$

where $T$ is the overpass time interval [days]. For an observation to be detected as an outlier, $\Delta innov_i$ should be larger than a certain threshold, expressed in dB. The latter is chosen to be adaptive, i.e. a multiple of the standard deviation of the innovations ($SD_{innov,n}$) computed on the antecedent $n$ days. The choice was made to dynamically compute $SD_{innov,n}$ with a moving window to account for the natural variability of the model and observation errors, and thus the innovations. In this study, the buddy check approach was tested for two different window sizes, i.e. windows of 20 ($SD_{innov,20}$) and 60 days ($SD_{innov,60}$) were considered. The outlier detection is illustrated in Figure 2b.

A strong positive innovation (outlier) hints towards an unmodeled process, i.e. irrigation. Therefore, when an outlier is detected at day $i$, irrigation can be triggered but only when the conditions required for irrigation are met: (1) the day $i$ has to fall in the growing season, and (2) the $MA$ should be lower than a certain threshold to avoid unrealistic irrigation events (when the soil is too wet). The latter threshold is set to 0.50 and is slightly

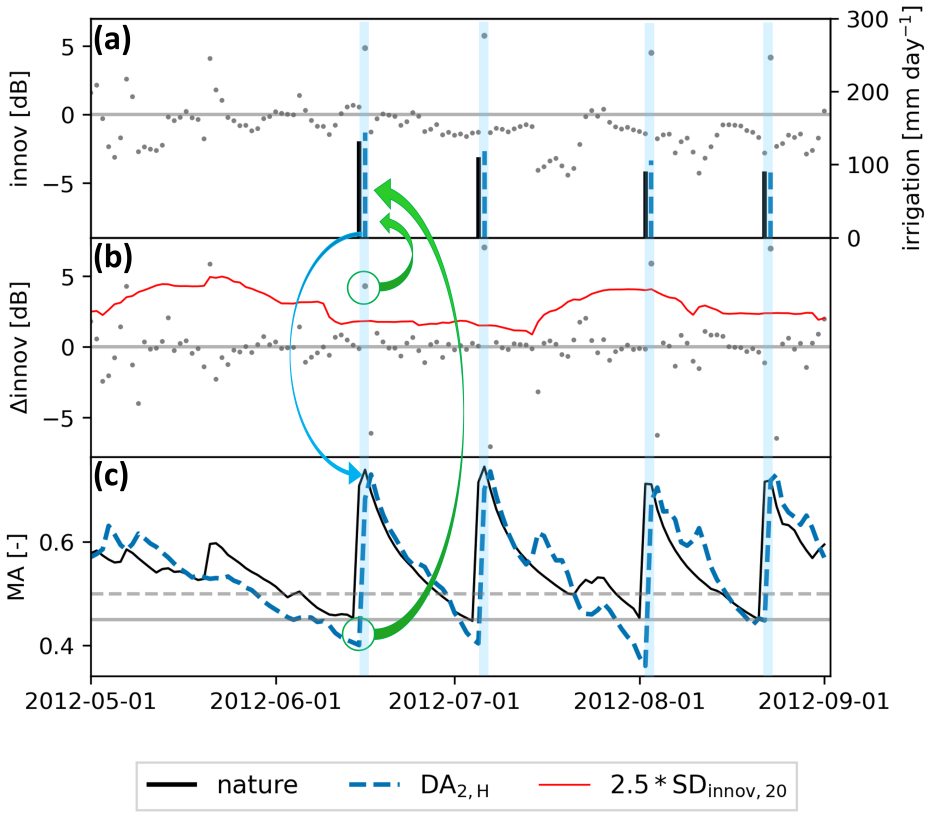


**Figure 2.** Illustration of the buddy check approach. (a) Irrigation time series [mm day$^{-1}$] of the nature run and the DA run with buddy check approach with the innovations [dB] in grey. (b) $\Delta innov$ [dB] time series with the dynamic threshold (based on a 20-day window, $2.5 * SD_{innov,20}$). (c) Moisture availability ($MA$ [-]) of the nature run and the DA buddy check run and the corresponding thresholds: 0.45 fixed threshold for irrigation for the nature run, 0.50 upper threshold to allow irrigation for the buddy check approach. The shaded blue stripes highlight the irrigation events. The green arrows illustrate the two conditions required to simulate irrigation. The blue arrow links the irrigation event to the increase in $MA$.

relaxed compared to the truth's 0.45 value to give way to an observation-based trigger, e.g. when a farmer would irrigate before the uncertain model reaches a critical $MA$. Furthermore, unlike the nature (or OL or $DA_1$ case), the $DA_2$ approach allows the $MA$ to decrease freely, mimicking the reality that farmers might sometimes irrigate later than expected. The condition on the $MA$ is illustrated by Figure 2c. For each irrigation event, the rootzone soil moisture is increased to field capacity, corresponding to $MA$=1. However, this is not visible in $MA$ time series (Figure 2c) as the plotted $MA$ is computed based on the daily averaged soil moisture contents. For days in the growing season (from April through September for the climatological GVF), the conditions to trigger irrigation can thus be summarized as follows:

$$\begin{cases} \Delta innov_i \geq 2.5 * SD_{innov,n} \\ MA_i \leq 0.50 \end{cases} \tag{8}$$

In short, an outlier innovation is not used to update the soil moisture state, but to correct the model input by adding water as irrigation. The amount of irrigation water is computed

by the irrigation scheme coupled to the Noah-MP LSM described in Section 2.1, and it benefits from the updated soil moisture prior to the irrigation trigger. It is important to note that this method was implemented in the LIS framework itself, allowing an online modeling of irrigation with this approach. However, since irrigation starts at 6:00 LT in the irrigation scheme, and the synthetic $\gamma^0_{VV}$ observations were produced at the same time of the day, irrigation is not yet part of the observations when they are checked for assimilation (and either assimilated or flagged as outlier): the irrigation of day $i$ is only visible in the observation of day $i+1$ (see Figure 2). Hence, with this buddy check approach, irrigation events are always delayed compared the truth. This technical detail is tied to observation and irrigation times, and could be overcome via postprocessing or model rewinding in the future.

### 2.5 Evaluation metrics

The experiments were evaluated in terms of irrigation, soil moisture, ET, and LAI. Soil moisture was assessed for the different layers (SSM, SM1, SM2, SM3) as defined in Section 2.1. The metrics used in this study to evaluate these variables are the Pearson correlation (R), the bias, and the root-mean-square difference (RMSD), and are defined as follows:

$$R = \frac{\sum_{n=1}^{N}(x_n - \bar{x})(y_n - \bar{y})}{\sqrt{\sum_{n=1}^{N}(x_n - \bar{x})^2 \sum_{n=1}^{N}(y_n - \bar{y})^2}} \tag{9}$$

$$bias = \frac{1}{N}\sum_{n=1}^{N}(x_n - y_n) \tag{10}$$

$$RMSD = \sqrt{\frac{1}{N}\sum_{n=1}^{N}(x_n - y_n)^2} \tag{11}$$

where $x$ is the value of the simulated land surface variable from the OL or DA experiment, $y$ is the reference value (from the nature run), and $N$ are the number of reference data in time ($n = 1, \ldots, N$). $\bar{x}$ and $\bar{y}$ represent the temporal mean values. For LAI, the R is computed on the anomalies ($anomR$), because this land surface variable has a clear climatological pattern and naturally results in high R values.

The normalized information contribution in R ($\text{NIC}_R$) and RMSD ($\text{NIC}_{RMSD}$) is commonly used to describe the improvement or degradation of the estimates compared to a model only (OL) run:

$$NIC_R = \frac{R_{DA} - R_{OL}}{1 - R_{OL}} \tag{12}$$

$$NIC_{RMSD} = \frac{RMSD_{OL} - RMSD_{DA}}{RMSD_{OL}} \tag{13}$$

Positive NIC values correspond to an improvement while a negative NIC indicates poorer estimations than those of the OL.

Irrigation is evaluated with the same metrics on a daily basis, but also considering different levels of smoothing where the antecedent $n$ daily irrigation amounts are averaged. Smoothing windows of different lengths ($n$ days) are considered to better grasp for which time intervals (e.g., daily, weekly, monthly) the irrigation events can be accurately simulated. Additionally, binary metrics are considered to assess the performance to detect (in terms of

timing) the irrigation events. The probability of detection (POD) and the false alarm ratio (FAR) are computed on a daily basis and were defined by Roebber (2009) as follows:

$$POD = \frac{TP}{TP + FN} \tag{14}$$

$$FAR = \frac{FP}{TP + FP} \tag{15}$$

where TP, FN, and FP are the true positive (detected), false negative (missed), and false positive (false) irrigation events. Both metrics range from 0 to 1 and should be equal to 1 and 0 for the POD and FAR, respectively, in an ideal case. Note that POD and FAR were computed on the daily irrigation estimates ± 1 day, therefore accounting for the technical delay of irrigation with the buddy check approach (see Section 2.4.2).

## 3 Results

### 3.1 $DA_1$: soil moisture updating can limit irrigation estimation

In the default DA experiments ($DA_1$), irrigation is primarily triggered when the modeled (or analysis) soil moisture deficit exceeds a threshold. The results are first presented for the $DA_{1,H}$, for which daily $\gamma^0_{VV}$ observations without noise were assimilated into a model forced by precipitation taken from another time period than the truth. Figure 3a illustrates some irrigation events of the nature run ('truth'), $OL_H$, and $DA_{1,H}$ along with the $\gamma^0_{VV}$ innovations. The corresponding $MA$ time series are shown in Figure 3b with the threshold that needs to be reached to trigger irrigation (0.45). First, it can be seen that the assimilation of $\gamma^0_{VV}$ observations brings the soil moisture, and consequently the $MA$, to a state that is closer to the nature run, moving the first irrigation event (in June) closer to the nature run compared to the OL. In contrast, the last irrigation event (in August) does not occur in the $DA_{1,H}$. The $MA$ of $DA_{1,H}$ does not reach the 0.45 threshold before the true event and the irrigation simulation is consequently prevented by updates to wetter soil moisture conditions as a result of large positive innovations (Figure 3).

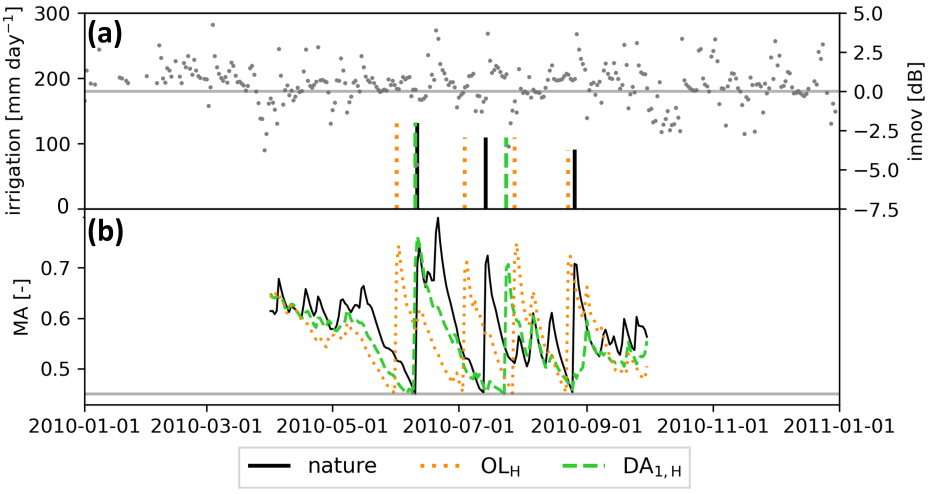


**Figure 3.** (a) Time series of the irrigation [mm day$^{-1}$] of the nature run, $OL_H$, and $DA_{1,H}$. The grey dots correspond to the $\gamma^0_{VV}$ innovations. (b) Time series of the corresponding moisture availability ($MA$ [-]) for the irrigation months (April through September) along with the corresponding threshold to trigger irrigation (grey line).

More generally, over the 10-year experiment, the DA irrigation events that are not estimated before the true irrigation are typically delayed or skipped, similar to what can be observed for July and August in Figure 3. For the 10-year period, the daily irrigation estimates ± 1 day have low POD values of 0.40 and 0.43 for $DA_{1,H}$ and $DA_{1,M}$, respectively. The system compensates for the lack of water in the soil through positive soil moisture increments instead of an irrigation application based on an improved initial condition. Figure 4 presents the effect of the assimilation on irrigation estimates in terms of NIC values for both forcing error ($DA_{1,H}$ and $DA_{1,M}$), along with the absolute metrics for the OL. Daily irrigation was smoothed for different window sizes before computing the $NIC_R$ and $NIC_{RMSD}$. For the $DA_1$ experiments (green), NIC values are positive for most smoothing intervals and peak when irrigation is smoothed over a 14-day window. However, the NIC metrics drop to negative values for $DA_{1,M}$ starting from a bimonthly smoothing. This can be explained by the difference in forcings. The ERA5 meteorology follows the seasonal patterns of the MERRA2 meteorology used for the truth, therefore the seasonal amount of irrigation from a model-only $OL_M$ run is close to the nature, as indicated by the high R and low RMSD values, especially for the longer aggregation windows in Figure 4c and d. The effect of (sometimes erroneous) irrigation estimation on other land surface variables is later discussed in Section 3.2.3.

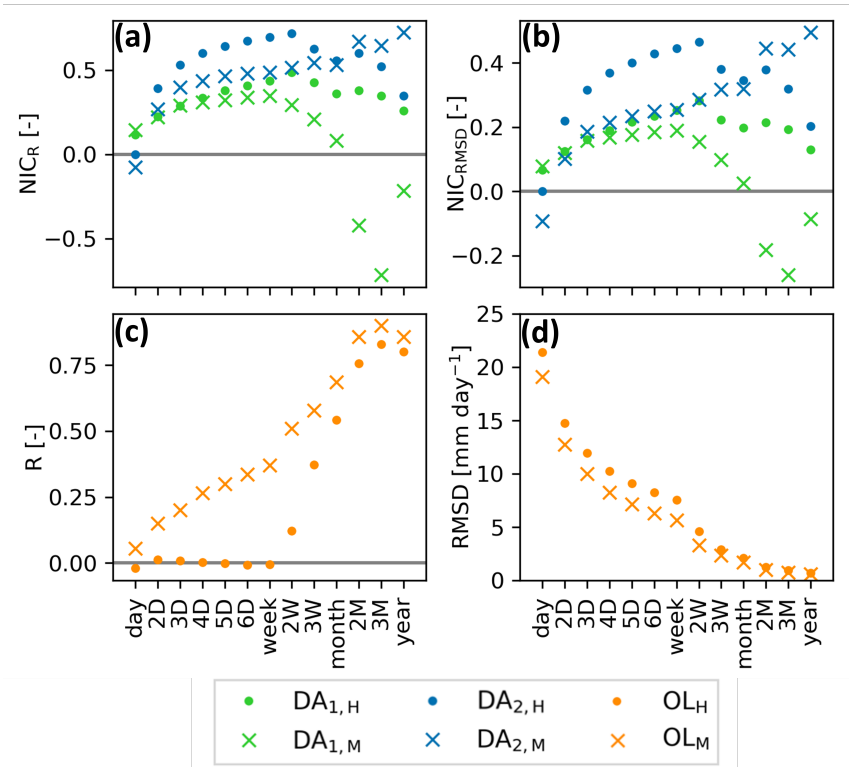


**Figure 4.** (a) $NIC_R$ [-] and (b) $NIC_{RMSD}$ [-] for irrigation smoothed with different window sizes. (c) Pearson R [-] and (d) RMSD [mm day$^{-1}$] of the OL. The dots and the crosses correspond to the high and mild forcing error experiments, respectively. $DA_2$ were performed by assimilating daily perfect observations. All metrics were computed on the irrigation months only (April through September) over the 10-year experiment.

The missed or delayed irrigation events can be identified in the innovation time series. Large innovations occur on true irrigation days (Figure 3a), highlighting that a process is missed by the model. Instead of avoiding or delaying the event in a DA run, the newly

proposed buddy check approach, for which the results are described in the next section, can identify and trigger such irrigation events.

### 3.2 $DA_2$: new buddy check approach

#### *3.2.1 Assimilation of daily perfect backscatter observations*

The results of the new buddy check approach are first presented for daily assimilation of observations without white noise and using a 20-day window to compute the outlier threshold ($SD_{innov,20}$). Figure 5 shows the innovations and irrigation results of $DA_{2,H}$ for the period 2010-2015 (panel a), with the associated $MA$ time series for 2010 in panel b. The $DA_{2,H}$ irrigation estimates (dashed blue bars) capture most of the true irrigation events (full black lines). During these five years, one event is missed at the end of the irrigation season in 2013. This can be explained by (intentionally) erroneous rainfall events in the DA run, causing soil moisture that is higher than the irrigation threshold ($MA > 0.5$). On the other hand, two false irrigation events are simulated. Both can be attributed to rainfall events in the nature run, leading to an occasional large positive innovation, and since the moisture conditions are dry enough, irrigation is consequently triggered. This proves that when the forcings are erroneous (i.e. rainfall is missed in the DA run), irrigation cannot be dissociated from rainfall in the $\gamma^0_{VV}$ signal.

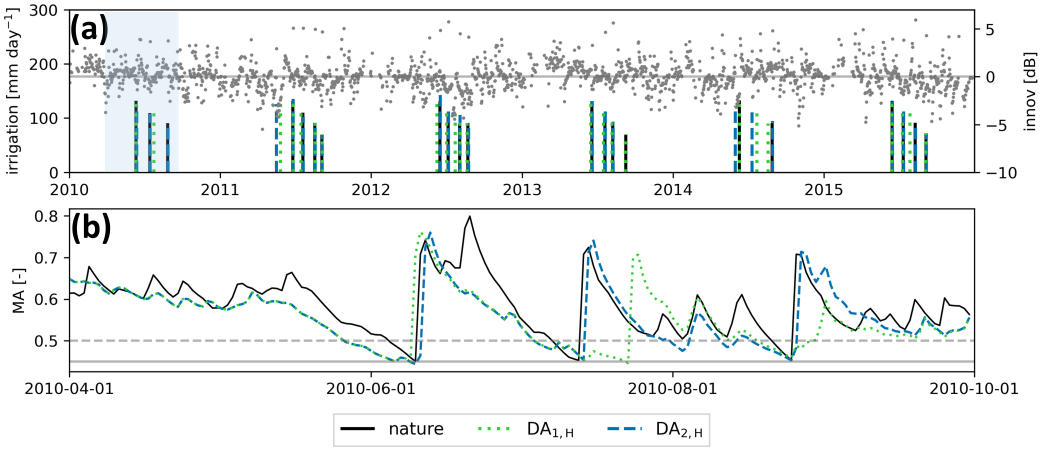


**Figure 5.** (a) Time series of the irrigation [mm day$^{-1}$] of the nature run, $DA_{1,H}$, and $DA_{2,H}$ for daily observations without noise and an outlier threshold based on $SD_{innov,20}$. Innovations of $DA_{2,H}$ are shown in the background in grey. (b) Time series for the growing season of 2010 (shaded in blue in a) of the moisture availability ($MA$ [-]) of the nature run, $DA_{1,H}$, and $DA_{2,H}$ for the irrigation months (April through September). In (b), the dashed grey line corresponds to the maximum allowable $MA$ for irrigation for $DA_{2,H}$ (0.50) and the full line is the threshold for the nature run and $DA_{1,H}$ (0.45).

Over the whole 10-year experiment, irrigation estimates are strongly improved by the implementation of the buddy check approach, raising the POD of the daily irrigation estimates ± 1 day from 0.40 for $DA_{1,H}$ to 0.86 for $DA_{2,H}$, and from 0.43 for $DA_{1,M}$ to 0.80 for $DA_{2,M}$. For both forcing errors, the FAR is about 0.17, which is also an improvement compared to the values for $DA_{1,H}$ (0.60) and $DA_{1,M}$ (0.42). Figure 4 shows the $NIC_R$ and $NIC_{RMSD}$ for the different irrigation smoothing windows for $DA_{2,H}$ and $DA_{2,M}$ (daily assimilation without noise). Unlike $DA_1$, the NIC values for all $DA_2$ experiments remain above the zero-line, meaning that irrigation estimates are improved for all smoothing intervals, relative to the OL. Starting from a 3-day smoothing interval, R and RMSD values are

improved by more than 30% and 10%, respectively, for all forcing errors and smoothing intervals. NIC values tend to drop for $DA_{2,H}$ for longer aggregation levels as a consequence of the occasional false or missed irrigation events. The poor effect on irrigation quantification at a daily scale can be attributed to the timing of the observation and irrigation application (see Section 2.4.2).

#### *3.2.2 Effect of observation interval and white noise*

The buddy check implementation was tested for different observation intervals (1, 2, 3, and 7 days) and observation noise levels (0, 0.3, 0.5, and 0.7 dB), to assess which observation configuration would be ideally suited for irrigation estimation. The 14-day smoothed daily $DA_2$ irrigation estimates are evaluated relative to the OL through the $NIC_R$ and $NIC_{RMSD}$. The bias (difference between the daily simulated and nature irrigation) is also assessed to indicate if there is a general over- or underestimation of the irrigation amounts. The results for the $DA_{2,H}$ and $DA_{2,M}$ experiments are shown in Figure 6. Two thresholds were tested to trigger irrigation, using two different window sizes for the calculation of $SD_{innov}$: 20 days ($SD_{innov,20}$), and 60 days ($SD_{innov,60}$). Note that the experiments assimilating observations with a 7-day interval could only be performed with a 60-day window in order to compute a standard deviation with enough data points. All experiments with white noise in the observation signal were performed for three random seeds of added noise and the average metric is presented.

The performance of the buddy check approach degrades with longer observation intervals, to reach marginal improvements for the $DA_{2,H}$, and even poorer irrigation estimations for the $DA_{2,M}$ than for $OL_M$ (Figure 6a,b,d,e). Less frequent observations lead to stronger underestimations of the irrigation amounts, as shown by the negative biases (Figure 6f). In the worst scenario for $DA_{2,H}$ (7-day observation interval with noise), about half of the true irrigation water is missing over the 10 years. Even though $DA_2$ misses more irrigation for larger observation intervals compared to the OL, the timing of the remaining detected irrigation events is closer to the truth.

The white noise in the signal mainly affects the performance when observations are frequently available (daily or once every 2 days) for $DA_{2,H}$ (Figure 6). Similar to the effect of a longer observation interval, noise in the signal tends to cause underestimations of irrigation amounts. White noise sometimes amplifies the increase in $\Delta innov$, making an outlier easier to detect, and at other times, the noise reduces the 'jump' effect, making the event undetectable. Observation noise also increases the risk of detecting a false irrigation event. The combination of these three effects reduces the skill of the buddy check approach. For reasonable levels of noise ($\leq$ 0.5 dB; Figure 6e), the RMSD is reduced by at least 30% when assimilating frequent observations, for both forcing errors.

Increasing the window size for the computation of the $SD_{innov}$ improves the R and RMSD for $DA_{2,M}$. However, it leads to irrigation underestimation (negative bias) for non-daily observations, especially in the case of the $DA_{2,H}$ (Figure 6f). More irrigation events remain undetected because the $SD_{innov}$ considers innovations up to 60 days before the event. This is problematic, especially at the beginning of the season as the natural variation in the innovations is larger in the late winter or spring (wet season), which are then considered in the computation of the $SD_{innov,60}$. On the other hand, a small window size ($SD_{innov,20}$) tends to detect more false irrigation events, keeping the bias closer to zero, but not necessarily improving the R and RMSD in terms of irrigation. A window size of 20 days seems more appropriate, in the sense that this $SD_{innov}$ should capture the natural variation of the innovations which is mainly induced by forcing errors but also vegetation.

Overall, NIC values for the $DA_{2,H}$ are larger than for the $DA_{2,M}$, in line with the larger forcing errors in $DA_{2,H}$. The $OL_M$ already shows a reasonable performance (Figure 4c,d), leaving less space for improvement by the $DA_{2,M}$.

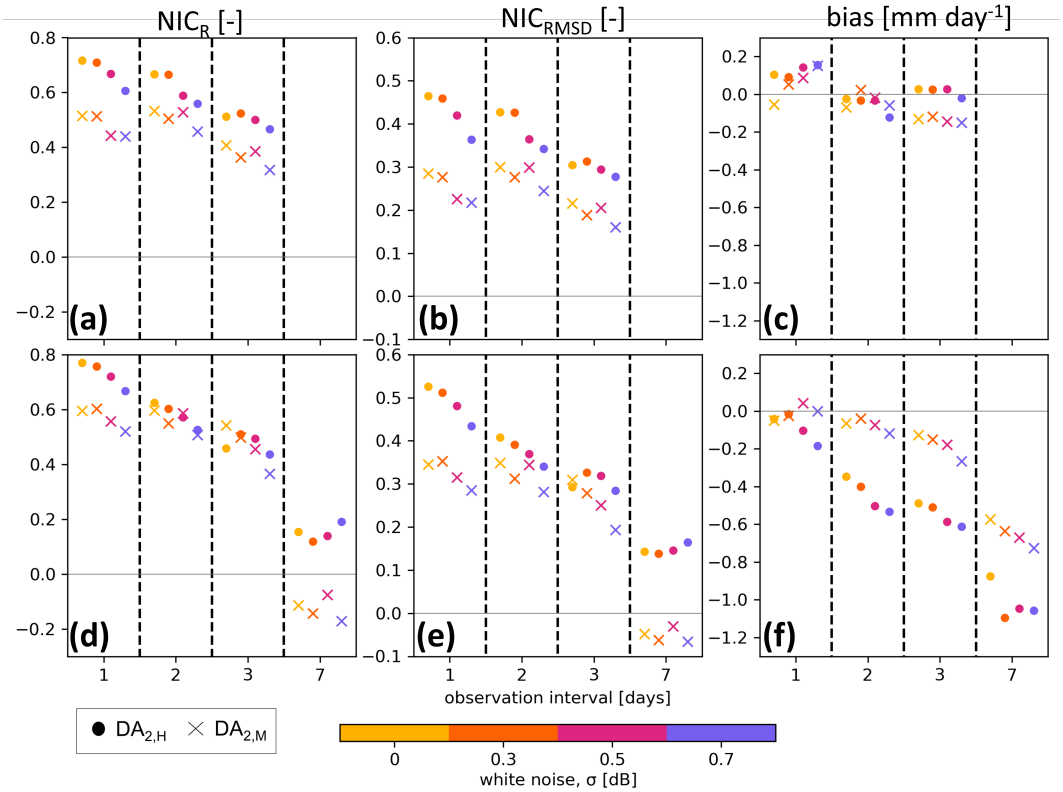


**Figure 6.** (a,d) NIC$_R$ [-], (b,e) NIC$_{RMSD}$ [-], and (c,d) bias [mm day$^{-1}$] of 14-day irrigation amount estimates for the different DA$_2$, for 1, 2, 3, and 7-day observation intervals. The colors correspond to the level of Gaussian white noise added to the signal ($\sigma$, dB), and for all experiments with noise, the mean metric is taken from the three runs. The rows are associated with the window size taken to compute the standard deviation for the irrigation threshold, where (a,b,c) are based on a 20-day window ($SD_{innov,20}$), and (d,e,f) relate to experiments with a 60-day window ($SD_{innov,60}$). Dots correspond to DA$_{2,H}$ and crosses to DA$_{2,M}$.

### *3.2.3 Impact on other land surface variables*

The quality of irrigation estimates has an impact on the other land surface variables. Table 1 shows the R values between daily results for selected OL and DA experiments, relative to the truth. The DA$_2$ results are shown for an outlier threshold based on $SD_{innov,60}$ (with irrigation underestimation, Figure 6f) to include the experiments for which weekly observations are assimilated. First, the difference between the two forcing errors is reflected in the significantly lower R values for OL$_H$ than for OL$_M$. For DA$_2$, it can be noticed that the novel buddy check approach using daily observations without noise (DA$_2$ 1 day, 0 dB) performs best and is clearly superior to the DA$_1$ (with daily, perfect observations). The R values of the DA$_2$ with a 3-day interval and 0.5 dB observation noise are close to those of the DA$_1$ for both the high and mild forcing error experiments. In the worst case evaluated in this study (7-day interval and 0.7 dB of noise), the performance remains better than the OL when forcings are strongly altered (DA$_{2,H}$), but under the same circumstances, the new method degrades the land surface estimates when forcings are only slightly changed (DA$_{2,M}$).

**Table 1.** R for the SSM, SM1, SM2, SM3, ET, and anomR for LAI, for selected experiments calculated on the entire 10-year experiment. All $DA_2$ were performed with the $SD_{innov,60}$ threshold.

| | SSM | SM1 | SM2 | SM3 | ET | LAI |
|---|---|---|---|---|---|---|
| | | | R [-] | | | anomR [-] |
| **High forcing error** | | | | | | |
| OL | 0.32 | 0.26 | 0.34 | 0.49 | 0.80 | -0.12 |
| $DA_1$ | 0.60 | 0.60 | 0.68 | 0.76 | 0.86 | 0.21 |
| $DA_2$ 1 day, 0 dB | 0.70 | 0.73 | 0.79 | 0.79 | 0.89 | 0.31 |
| $DA_2$ 3 day, 0.5 dB | 0.56 | 0.53 | 0.57 | 0.65 | 0.83 | 0.17 |
| $DA_2$ 7 day, 0.7 dB | 0.49 | 0.45 | 0.52 | 0.60 | 0.78 | -0.01 |
| **Mild forcing error** | | | | | | |
| OL | 0.73 | 0.69 | 0.71 | 0.82 | 0.88 | 0.71 |
| $DA_1$ | 0.82 | 0.81 | 0.81 | 0.89 | 0.91 | 0.78 |
| $DA_2$ 1 day, 0 dB | 0.86 | 0.84 | 0.88 | 0.93 | 0.92 | 0.88 |
| $DA_2$ 3 day, 0.5 dB | 0.79 | 0.76 | 0.79 | 0.87 | 0.90 | 0.84 |
| $DA_2$ 7 day, 0.7 dB | 0.72 | 0.66 | 0.66 | 0.80 | 0.86 | 0.60 |

For longer observation intervals, the anomR of LAI reduces significantly in the $DA_2$ runs. When irrigation events are missed in the new $DA_2$ system (e.g. because the next observation falls too far in time after the irrigation event, making irrigation undetectable in the signal), there is a risk that LAI starts to drop drastically as a response to a water shortage in the root zone.

## 4 Discussion

### 4.1 Novel approach to estimate irrigation in a DA system

The synthetic setup in this study helps to optimize the DA design for irrigation quantification. The soil moisture updating via DA can help to improve the initial conditions to trigger irrigation and to estimate the right amount of irrigation, but a blind ingestion of all observations can update soil moisture to wetter conditions which already reflect the presence of irrigation and inhibit irrigation estimation by the model, as in Modanesi et al. (2022). This phenomenon was illustrated in Figure 3 where irrigation events were delayed or missed because the required water is compensated by strong positive soil moisture increments. The idea of the buddy check approach builds on this limitation by preventing these updates to wetter conditions and forcing irrigation in the model instead. More specifically, the method relies on the fact that a sudden large difference between the observed and forecasted $\gamma^0_{VV}$ can only come from an unmodeled process, which corresponds to irrigation in this synthetic experiment. The primary condition is now the detection of an outlier (observation-based) and not the soil moisture deficit threshold anymore. This makes the timing of the estimated irrigation less model-dependent and more in line with actual practices on the field.

The new method shows good performances in terms of irrigation estimation when frequent (daily or every other day) observations are available, which corresponds to the initial revisit interval (2-3 days, location dependent) of the S1 constellation over Europe. Reasonable performances are still expected for a 3-day observation interval but weekly observations would not be sufficient to guarantee the irrigation detection skill and lead to severe underestimations of irrigation water. The failure of S1-B halved the number of available observations (one every ∼4 days in Europe, 12 days elsewhere), making the buddy check approach (used within a S1 DA system) unsuitable outside of Europe until the launch of the next satellite

(S1-C, expected in the spring of 2023). Other synthetic studies assimilating S1-related SSM products (Abolafia-Rosenzweig et al., 2019; Das et al., in review; Ouaadi et al., 2021; Zappa et al., 2022) also highlighted the importance of frequent observations. Zappa et al. (2022) reported large irrigation underestimations when observations are too sparse in time. Similar to our study using $\Delta innov$ to detect outliers, their approach is based on observed differences in soil moisture ($\Delta SM$). Both methods are observation-based, making them sensitive to observation noise, and to underestimation of the irrigation amounts with less frequent observations, because the irrigation signal fades away in the observations with time. In short, our buddy check approach underestimates irrigation more for infrequent observations or when a large time window is used to compute the $\Delta innov$ threshold ($SD_{innov,60}$), but the remaining detected irrigation events are identified accurately in time and with the correct amounts of irrigation water.

The main advantages of the new buddy check approach are (1) the flexibility of the outlier detection method to different situations (and different errors), and (2) the relaxation of the model-based soil moisture threshold for irrigation, making the irrigation estimates more in line with what happens in reality (as observed by the satellite). First, the standard deviation of the $\gamma^0_{VV}$ innovations for the $\text{DA}_H$ and $\text{DA}_M$ experiments reach average values of 1.5 dB and 1 dB, respectively, for the adaptive outlier detection (Equation 8) during the growing season. These values are in line with the magnitude of the expected high and mild forcing errors, with precipitation RMSD values of 5.1 mm day$^{-1}$ and 3.6 mm day$^{-1}$, respectively. Consequently, the DA results for both experiments were comparable in terms of NIC. It is expected that the threshold will also adapt to the location (i.e. the soil texture, crop type), which avoids the use of location-dependent thresholds (i.e. a new parameter) for the outlier detection. Second, setting an upper boundary to the $MA$ to allow irrigation is more realistic than the use of a fixed threshold. For irrigation to be triggered, the threshold can slightly be higher (wetter, up to 0.50 in this case) or much lower (drier). This is more in line with a real world situation where irrigation is not necessarily determined by a fixed soil moisture deficit value, but depends on the agricultural practices and more generally on the water availability.

### 4.2 Limitations and opportunities

The main limitation of the buddy check approach is the missing of irrigation events, esp. for longer observation intervals. To counter this problem, we need frequent satellite data or a hybrid DA system, where the buddy check approach is supplemented with a pure MA-based irrigation model trigger, if the observation interval exceeds the surface soil memory of an irrigation event. The missed irrigation events have the strongest impact on vegetation, with a steep decline in LAI. This issue can be tackled by jointly updating SSM and LAI, as done by Modanesi et al. (2022). Vegetation updating would ask for the assimilation of backscatter in cross-polarization ($\gamma^0_{VH}$) as this signal has shown to be more affected by vegetation (Patel et al., 2006; Vreugdenhil et al., 2018). A joint assimilation of $\gamma^0_{VV}$ and $\gamma^0_{VH}$ would require a combination of both innovations in our buddy check method approach.

The newly proposed buddy check approach could also be used to estimate irrigation with other (e.g. particle) filters or other observations than backscatter data. High resolution L-band soil moisture data would be interesting to guide the estimation of irrigation amounts. Such data can be obtained from e.g., downscaled SMOS or AMSR-E with DisPATCh (Malbéteau et al., 2016) or future missions such as the Copernicus ROSE-L (Davidson & Furnell, 2021) and the SMOS-HR (Rodríguez-Fernández et al., 2019). Nevertheless, the outcome would strongly depend on the quality of the retrievals, and an appropriate bias treatment is needed to avoid the attenuation of the irrigation in the signal (Kumar et al., 2015; Kwon et al., 2022). Instead of changing the type of assimilated observations, the buddy check method could also be used in systems with other models, possibly crop models that are originally designed for agriculture, offering new opportunities in such fields of application.

### 4.3 Future real world experiment

The success of a real world DA experiment with the buddy check approach will depend on the observability of irrigation and model-related limitations. First, satellite observations need to be available at high spatial and temporal resolution, and the actual type of irrigation method needs to be detectable. There is a chance that irrigation is applied for consecutive days over different fractions of the observed satellite footprint (one or a few fields receive irrigation per day). In that case, 'jumps' in the innovations will not be detected and the backscatter signal is likely to remain high for these consecutive days. Future research is necessary to counter this limitation, or higher resolution input data and observations are needed. Similarly, some types of irrigation will be easy to detect, whereas others not. Punctual large sprinkler events, as simulated in this study, are more easily detectable than e.g., drip irrigation, which is typically applied in smaller amounts and more frequently.

Second, the LSM and WCM are assumed to be perfect in our synthetic study, but the model-related limitations already mentioned in Modanesi et al. (2022) will be important when going to a real world experiment. Concerning the LSM, the quality of the input data is crucial. Erroneous crop rooting depth, soil texture, or irrigation fraction, would automatically lead to a bias in the irrigation amounts since these factors directly influence the volumes of irrigation water (see LSM equations in Section 2.1). Though more flexible than a rigid soil moisture deficit threshold to trigger irrigation, the upper $MA$ threshold of the buddy check approach (set to 0.50 in this study) will need some calibration, as this value may vary across regions. Also the reliability of meteorological forcings is essential. As demonstrated by $DA_2$, an outlier can occur when there was a true precipitation event that was not included in the forcings of the simulation (Figure 5). When the root zone is dry enough to allow irrigation, these precipitation events (typically larger than 10 mm) cannot be distinguished from an irrigation event in the signal. The observation operator (e.g. WCM) could also pose a limitation, when directly assimilating microwave signals. Rather than calibrating an empirical model, novel machine-learning based observation operators could improve the system (de Roos et al., in review; Rains et al., 2022), but in both cases, the observation operator training might suffer from an inaccurate match between irrigation simulation (and the effect on soil moisture) and irrigation observed in the satellite signals.

## 5 Conclusions

Irrigation detection and quantification are major challenges. New methods based on remote sensing data are now emerging, including the use of microwave observations in combination with models through data assimilation (DA). Modanesi et al. (2022) assimilated Sentinel-1 backscatter observations into the Noah-MP version 3.6, coupled to a sprinkler irrigation scheme. The soil moisture and vegetation state were updated to set better initial conditions to trigger irrigation simulation, but the system also had limitations, esp. when large updates to wetter conditions delayed or completely inhibited the process-based modeling of irrigation events. This hampers the irrigation quantification by the process model.

In this study, we conducted synthetic experiments for the assimilation of backscatter observations ($\gamma^0_{VV}$) to update soil moisture in a system with erroneous meteorological forcings. After illustrating the shortcoming of blindly assimilating all data for state updating, a new method was developed based on a buddy check approach, in which innovation (observation *minus* forecast) outliers are detected and not assimilated. The method still updates the land surface to guarantee the best possible initial conditions to estimate irrigation amounts, but when an outlier in the innovations is detected, an unmodeled process is assumed and the large innovation is not assimilated. Consequently, the 'missed' irrigation is triggered, if the rootzone soil moisture is dry and it is a day in the growing season. The new method is now primarily observation-based, and better adapts to the timing of real irrigation events. The threshold value to identify outlier innovations was made dependent on the locally and

temporally varying errors in the system. The method was tested for several observation intervals (1, 2, 3, and 7 days) and levels of observation noise, added as Gaussian white noise of mean zero and variable standard deviations (0, 0.3, 0.5, and 0.7 dB). The main results can be summarized as follows:

1. For biweekly aggregated irrigation estimates, and compared to a model-only run, the new DA method reaches 50–80% and 20–50% of improvement in terms of Pearson R and RMSD, respectively, when frequent observations (daily or every other day) are available. From a 3-day observation interval onward, the performance degrades but remains reasonable ($NIC_R$: 20–40%, $NIC_{RMSD}$: 15–35%), and for weekly observations, there is no improvement compared to a model-only run ($NIC_R$: -10–10%, $NIC_{RMSD}$: -10–15%).
2. The largest improvements from the DA can be seen when the forcing error is large (strongly altered meteorological forcings) with a maximum performance for a biweekly aggregation of irrigation. When forcing errors are mild (meteorological forcings closer to the truth), the improvement peaks for the seasonal irrigation estimates.
3. Observation error has less impact on the irrigation estimations than the observation interval. The $NIC_R$ drops on average by $\sim$10% when going from perfect observations to random noise levels with a standard deviation of 0.7 dB. Noise negatively impacts the performance, especially for frequent observations where irrigation events remain undetected or false events are encountered.
4. The DA improves other land surface variables, such as soil moisture, ET, or LAI along with the irrigation estimates. However, the DA cannot recover the LAI when the assimilated observations are too sparse in time. The LAI drops as a response to the dry soil moisture when irrigation events are missed.

The adaptive buddy check approach is flexible and offers new opportunities. The method was tested for two very different sets of erroneous forcings and the results were similar in terms of improvement compared to a model-only run, suggesting that the method indeed adapts to different situations. Furthermore, the buddy check approach can easily be implemented in other systems: with another assimilated product (high resolution soil moisture retrievals) or with another LSM (or a crop model). After this synthetic evaluation of the method, the system is ready to be tested in the real world, but future developments (e.g. a hybrid observation- and model-based triggering of irrigation, in case of infrequent observations) will be required to obtain a mature DA system for irrigation estimation. The localized nature of irrigation in space and time asks for high resolution satellite data, efficient modeling, and continued DA advances to accurately quantify the most important human use of water.

## 6 Open Research

The new method implemented in the Land Information System version 3.4 will be made available on GitHub after acceptance of this paper, along with the output of the synthetic experiment runs in the form of netCDF files, that will be published on Zenodo. The code and data can be provided during the review process upon request to the author.

The LIS parameters and source code are freely available at `https://lis.gsfc.nasa.gov/` and `https://github.com/NASA-LIS/LISF`. The MERRA-2 data (Gelaro et al., 2017) were obtained from: `https://goldsmr4.gesdisc.eosdis.nasa.gov/data/MERRA2/`. In order to access the data, an account at `https://urs.earthdata.nasa.gov/home` is needed. The ERA5 data used in this study have been processed and provided by Météo-France. Publicly available ERA5 data can be accessed via the Copernicus Climate Data Store at `https://cds.climate.copernicus.eu/` (Hersbach et al., 2020).

**Acknowledgments**

The research was funded by the Research Foundation – Flanders (FWO; grant no. 1158423N), ESA IRRIGATION+ (contract no. 4000129870/20/I-NB) and internal KU Leuven C1 (C14/21/057). The resources and services used in this work were provided by the VSC (Flemish Supercomputer Center), funded by the FWO and the Flemish government.

## References

Abolafia-Rosenzweig, R., Livneh, B., Small, E., & Kumar, S. (2019). Soil Moisture Data Assimilation to Estimate Irrigation Water Use. *Journal of Advances in Modeling Earth Systems*, *11*(11), 3670–3690. Retrieved 2022-05-03, from https://onlinelibrary.wiley.com/doi/abs/10.1029/2019MS001797 (_eprint: https://onlinelibrary.wiley.com/doi/pdf/10.1029/2019MS001797) doi: 10.1029/2019MS001797

Allen, R. G., Pereira, L. S., Raes, D., & Smith, M. (1998). FAO Irrigation and drainage paper No. 56. *Rome: Food and Agriculture Organization of the United Nations*, *56*(97), e156.

Attema, E. P. W., & Ulaby, F. T. (1978). Vegetation modeled as a water cloud. *Radio Science*, *13*(2), 357–364. Retrieved 2021-02-25, from https://agupubs.onlinelibrary.wiley.com/doi/abs/10.1029/RS013i002p00357 (_eprint: https://agupubs.onlinelibrary.wiley.com/doi/pdf/10.1029/RS013i002p00357) doi: 10.1029/RS013i002p00357

Bauer-Marschallinger, B., Freeman, V., Cao, S., Paulik, C., Schaufler, S., Stachl, T., ... Wagner, W. (2019, January). Toward Global Soil Moisture Monitoring With Sentinel-1: Harnessing Assets and Overcoming Obstacles. *IEEE Transactions on Geoscience and Remote Sensing*, *57*(1), 520–539. (Conference Name: IEEE Transactions on Geoscience and Remote Sensing) doi: 10.1109/TGRS.2018.2858004

Bazzi, H., Baghdadi, N., Fayad, I., Charron, F., Zribi, M., & Belhouchette, H. (2020, January). Irrigation Events Detection over Intensively Irrigated Grassland Plots Using Sentinel-1 Data. *Remote Sensing*, *12*(24), 4058. Retrieved 2021-10-20, from https://www.mdpi.com/2072-4292/12/24/4058 (Number: 24 Publisher: Multidisciplinary Digital Publishing Institute) doi: 10.3390/rs12244058

Bazzi, H., Baghdadi, N., Fayad, I., Zribi, M., Belhouchette, H., & Demarez, V. (2020, January). Near Real-Time Irrigation Detection at Plot Scale Using Sentinel-1 Data. *Remote Sensing*, *12*(9), 1456. Retrieved 2021-10-20, from https://www.mdpi.com/2072-4292/12/9/1456 (Number: 9 Publisher: Multidisciplinary Digital Publishing Institute) doi: 10.3390/rs12091456

Bonfils, C., & Lobell, D. (2007, August). Empirical evidence for a recent slowdown in irrigation-induced cooling. *Proceedings of the National Academy of Sciences*, *104*(34), 13582–13587. Retrieved 2021-10-11, from https://www.pnas.org/content/104/34/13582 (Publisher: National Academy of Sciences Section: Physical Sciences) doi: 10.1073/pnas.0700144104

Bretreger, D., Yeo, I.-Y., & Hancock, G. (2022, February). Quantifying irrigation water use with remote sensing: Soil water deficit modelling with uncertain soil parameters. *Agricultural Water Management*, *260*, 107299. Retrieved 2022-11-08, from https://www.sciencedirect.com/science/article/pii/S037837742100576X doi: 10.1016/j.agwat.2021.107299

Brocca, L., Ciabatta, L., Massari, C., Moramarco, T., Hahn, S., Hasenauer, S., ... Levizzani, V. (2014). Soil as a natural rain gauge: Estimating global rainfall from satellite soil moisture data. *Journal of Geophysical Research: Atmospheres*, *119*(9), 5128–5141. Retrieved 2022-11-07, from https://onlinelibrary.wiley.com/doi/abs/10.1002/2014JD021489 (_eprint: https://onlinelibrary.wiley.com/doi/pdf/10.1002/2014JD021489) doi: 10.1002/2014JD021489

Brocca, L., Tarpanelli, A., Filippucci, P., Dorigo, W., Zaussinger, F., Gruber, A., &

Fernández-Prieto, D. (2018, December). How much water is used for irrigation? A new approach exploiting coarse resolution satellite soil moisture products. *International Journal of Applied Earth Observation and Geoinformation*, *73*, 752–766. Retrieved 2022-11-04, from https://www.sciencedirect.com/science/article/pii/S0303243418304793 doi: 10.1016/j.jag.2018.08.023

Brombacher, J., Silva, I. R. d. O., Degen, J., & Pelgrum, H. (2022, June). A novel evapotranspiration based irrigation quantification method using the hydrological similar pixels algorithm. *Agricultural Water Management*, *267*, 107602. Retrieved 2022-11-07, from https://www.sciencedirect.com/science/article/pii/S0378377422001494 doi: 10.1016/j.agwat.2022.107602

Busschaert, L., de Roos, S., Thiery, W., Raes, D., & De Lannoy, G. J. M. (2022, July). Net irrigation requirement under different climate scenarios using AquaCrop over Europe. *Hydrology and Earth System Sciences*, *26*(14), 3731–3752. Retrieved 2022-10-27, from https://hess.copernicus.org/articles/26/3731/2022/ (Publisher: Copernicus GmbH) doi: 10.5194/hess-26-3731-2022

Cook, B. I., Shukla, S. P., Puma, M. J., & Nazarenko, L. S. (2015, March). Irrigation as an historical climate forcing. *Climate Dynamics*, *44*(5), 1715–1730. Retrieved 2021-11-19, from https://doi.org/10.1007/s00382-014-2204-7 doi: 10.1007/s00382-014-2204-7

Dari, J., Brocca, L., Modanesi, S., Massari, C., Tarpanelli, A., Barbetta, S., ... Volden, E. (in review). Regional data sets of high-resolution (1 and 6 km) irrigation estimates from space. *Earth System Science Data Discussions*, 1–34. Retrieved 2023-01-23, from https://essd.copernicus.org/preprints/essd-2022-403/ (Publisher: Copernicus GmbH) doi: 10.5194/essd-2022-403

Dari, J., Brocca, L., Quintana-Seguí, P., Escorihuela, M. J., Stefan, V., & Morbidelli, R. (2020, January). Exploiting High-Resolution Remote Sensing Soil Moisture to Estimate Irrigation Water Amounts over a Mediterranean Region. *Remote Sensing*, *12*(16), 2593. Retrieved 2021-10-20, from https://www.mdpi.com/2072-4292/12/16/2593 (Number: 16 Publisher: Multidisciplinary Digital Publishing Institute) doi: 10.3390/rs12162593

Das, N. N., Entekhabi, D., Dunbar, R. S., Chaubell, M. J., Colliander, A., Yueh, S., ... Thibeault, M. (2019, November). The SMAP and Copernicus Sentinel 1A/B microwave active-passive high resolution surface soil moisture product. *Remote Sensing of Environment*, *233*, 111380. Retrieved 2022-11-23, from https://www.sciencedirect.com/science/article/pii/S0034425719303992 doi: 10.1016/j.rse.2019.111380

Das, N. N., Jalilvand, E., Abolafia-Rosenzweig, R., Tajrishy, M., Kumar, S., & Mohammadi, M. R. (in review). Is it Possible to Quantify Irrigation Water-Use by Assimilating a High-Resolution Soil Moisture Product? *Authorea*. Retrieved 2022-11-07, from https://essopenarchive.org/doi/full/10.1002/essoar.10512082.1 doi: 10.1002/essoar.10512082.1

Davidson, M. W. J., & Furnell, R. (2021, July). ROSE-L: Copernicus L-Band Sar Mission. In *2021 IEEE International Geoscience and Remote Sensing Symposium IGARSS* (pp. 872–873). (ISSN: 2153-7003) doi: 10.1109/IGARSS47720.2021.9554018

Dee, D. P., Rukhovets, L., Todling, R., da Silva, A. M., & Larson, J. W. (2001). An adaptive buddy check for observational quality control. *Quarterly Journal of the Royal Meteorological Society*, *127*(577), 2451–2471. Retrieved 2022-11-23, from https://onlinelibrary.wiley.com/doi/abs/10.1002/qj.49712757714 (_eprint: https://onlinelibrary.wiley.com/doi/pdf/10.1002/qj.49712757714) doi: 10.1002/qj.49712757714

De Lannoy, G. J. M., Bechtold, M., Albergel, C., Brocca, L., Calvet, J.-C., Carrassi, A., ... Steele-Dunne, S. (2022). Perspective on satellite-based land data assimilation to estimate water cycle components in an era of advanced data availability and model sophistication. *Frontiers in Water*, *4*. Retrieved 2022-11-03, from https://www.frontiersin.org/articles/10.3389/frwa.2022.981745

de Roos, S., Busschaert, L., Lievens, H., Bechtold, M., & De Lannoy, G. J. M. (in review).

Optimisation and uncertainty assessment of AquaCrop backscatter simulations using Sentinel-1 observations. *Remote Sensing of Environment*.

Droogers, P., Immerzeel, W. W., & Lorite, I. J. (2010, September). Estimating actual irrigation application by remotely sensed evapotranspiration observations. *Agricultural Water Management*, *97*(9), 1351–1359. Retrieved 2022-11-08, from https://www.sciencedirect.com/science/article/pii/S0378377410001149 doi: 10.1016/j.agwat.2010.03.017

Döll, P. (2002, August). Impact of Climate Change and Variability on Irrigation Requirements: A Global Perspective. *Climatic Change*, *54*(3), 269–293. Retrieved 2021-09-28, from https://doi.org/10.1023/A:1016124032231 doi: 10.1023/A:1016124032231

Fischer, G., Tubiello, F. N., van Velthuizen, H., & Wiberg, D. A. (2007, September). Climate change impacts on irrigation water requirements: Effects of mitigation, 1990–2080. *Technological Forecasting and Social Change*, *74*(7), 1083–1107. Retrieved 2021-10-01, from https://www.sciencedirect.com/science/article/pii/S0040162506001429 doi: 10.1016/j.techfore.2006.05.021

Foley, J. A., Ramankutty, N., Brauman, K. A., Cassidy, E. S., Gerber, J. S., Johnston, M., ... Zaks, D. P. M. (2011, October). Solutions for a cultivated planet. *Nature*, *478*(7369), 337–342. Retrieved 2022-11-03, from https://www.nature.com/articles/nature10452 (Number: 7369 Publisher: Nature Publishing Group) doi: 10.1038/nature10452

Gelaro, R., McCarty, W., Suárez, M. J., Todling, R., Molod, A., Takacs, L., ... Zhao, B. (2017, July). The Modern-Era Retrospective Analysis for Research and Applications, Version 2 (MERRA-2). *Journal of Climate*, *30*(14), 5419–5454. Retrieved 2022-02-04, from https://journals.ametsoc.org/view/journals/clim/30/14/jcli-d-16-0758.1.xml (Publisher: American Meteorological Society Section: Journal of Climate) doi: 10.1175/JCLI-D-16-0758.1

Girotto, M., Reichle, R., Rodell, M., & Maggioni, V. (2021, January). Data Assimilation of Terrestrial Water Storage Observations to Estimate Precipitation Fluxes: A Synthetic Experiment. *Remote Sensing*, *13*(6), 1223. Retrieved 2022-05-16, from https://www.mdpi.com/2072-4292/13/6/1223 (Number: 6 Publisher: Multidisciplinary Digital Publishing Institute) doi: 10.3390/rs13061223

Gleick, P. H., Cooley, H., Morikawa, M., Morrison, J., & Cohen, M. J. (2009). *The World's Water 2008-2009: The Biennial Report on Freshwater Resources*. Island Press. (Google-Books-ID: lyG8BwAAQBAJ)

Gormley-Gallagher, A. M., Sterl, S., Hirsch, A. L., Seneviratne, S. I., Davin, E. L., & Thiery, W. (2022, February). Agricultural management effects on mean and extreme temperature trends. *Earth System Dynamics*, *13*(1), 419–438. Retrieved 2022-11-08, from https://esd.copernicus.org/articles/13/419/2022/ (Publisher: Copernicus GmbH) doi: 10.5194/esd-13-419-2022

Gutman, G., & Ignatov, A. (1998, January). The derivation of the green vegetation fraction from NOAA/AVHRR data for use in numerical weather prediction models. *International Journal of Remote Sensing*, *19*(8), 1533–1543. Retrieved 2022-11-16, from https://doi.org/10.1080/014311698215333 (Publisher: Taylor & Francis _eprint: https://doi.org/10.1080/014311698215333) doi: 10.1080/014311698215333

Hersbach, H., Bell, B., Berrisford, P., Hirahara, S., Horányi, A., Muñoz-Sabater, J., ... Thépaut, J.-N. (2020). The ERA5 global reanalysis. *Quarterly Journal of the Royal Meteorological Society*, *146*(730), 1999–2049. Retrieved 2022-11-24, from https://onlinelibrary.wiley.com/doi/abs/10.1002/qj.3803 (_eprint: https://onlinelibrary.wiley.com/doi/pdf/10.1002/qj.3803) doi: 10.1002/qj.3803

Hirsch, A. L., Wilhelm, M., Davin, E. L., Thiery, W., & Seneviratne, S. I. (2017). Can climate-effective land management reduce regional warming? *Journal of Geophysical Research: Atmospheres*, *122*(4), 2269–2288. Retrieved 2022-11-03, from https://onlinelibrary.wiley.com/doi/abs/10.1002/2016JD026125 (_eprint: https://onlinelibrary.wiley.com/doi/pdf/10.1002/2016JD026125) doi: 10.1002/2016JD026125

Jalilvand, E., Tajrishy, M., Ghazi Zadeh Hashemi, S. A., & Brocca, L. (2019, September). Quantification of irrigation water using remote sensing of soil moisture in a semi-arid region. *Remote Sensing of Environment*, *231*, 111226. Retrieved 2022-04-26, from https://www.sciencedirect.com/science/article/pii/S0034425719302457 doi: 10.1016/j.rse.2019.111226

Jin, N., Tao, B., Ren, W., Feng, M., Sun, R., He, L., ... Yu, Q. (2016, March). Mapping Irrigated and Rainfed Wheat Areas Using Multi-Temporal Satellite Data. *Remote Sensing*, *8*(3), 207. Retrieved 2022-11-04, from https://www.mdpi.com/2072-4292/8/3/207 (Number: 3 Publisher: Multidisciplinary Digital Publishing Institute) doi: 10.3390/rs8030207

Kumar, S. V., Peters-Lidard, C. D., Santanello, J. A., Reichle, R. H., Draper, C. S., Koster, R. D., ... Jasinski, M. F. (2015, November). Evaluating the utility of satellite soil moisture retrievals over irrigated areas and the ability of land data assimilation methods to correct for unmodeled processes. *Hydrology and Earth System Sciences*, *19*(11), 4463–4478. Retrieved 2022-05-03, from https://hess.copernicus.org/articles/19/4463/2015/ (Publisher: Copernicus GmbH) doi: 10.5194/hess-19-4463-2015

Kumar, S. V., Peters-Lidard, C. D., Tian, Y., Houser, P. R., Geiger, J., Olden, S., ... Sheffield, J. (2006, October). Land information system: An interoperable framework for high resolution land surface modeling. *Environmental Modelling & Software*, *21*(10), 1402–1415. Retrieved 2022-11-09, from https://www.sciencedirect.com/science/article/pii/S1364815205001283 doi: 10.1016/j.envsoft.2005.07.004

Kumar, S. V., Reichle, R. H., Peters-Lidard, C. D., Koster, R. D., Zhan, X., Crow, W. T., ... Houser, P. R. (2008, November). A land surface data assimilation framework using the land information system: Description and applications. *Advances in Water Resources*, *31*(11), 1419–1432. Retrieved 2022-11-09, from https://www.sciencedirect.com/science/article/pii/S0309170808000146 doi: 10.1016/j.advwatres.2008.01.013

Kwon, Y., Kumar, S. V., Navari, M., Mocko, D. M., Kemp, E. M., Wegiel, J. W., ... Bindlish, R. (2022, July). Irrigation characterization improved by the direct use of SMAP soil moisture anomalies within a data assimilation system. *Environmental Research Letters*, *17*(8), 084006. Retrieved 2022-09-21, from https://doi.org/10.1088/1748-9326/ac7f49 (Publisher: IOP Publishing) doi: 10.1088/1748-9326/ac7f49

Le Page, M., Berjamy, B., Fakir, Y., Bourgin, F., Jarlan, L., Abourida, A., ... Chehbouni, G. (2012, September). An Integrated DSS for Groundwater Management Based on Remote Sensing. The Case of a Semi-arid Aquifer in Morocco. *Water Resources Management*, *26*(11), 3209–3230. Retrieved 2022-11-08, from https://doi.org/10.1007/s11269-012-0068-3 doi: 10.1007/s11269-012-0068-3

Magidi, J., Nhamo, L., Mpandeli, S., & Mabhaudhi, T. (2021, January). Application of the Random Forest Classifier to Map Irrigated Areas Using Google Earth Engine. *Remote Sensing*, *13*(5), 876. Retrieved 2022-11-04, from https://www.mdpi.com/2072-4292/13/5/876 (Number: 5 Publisher: Multidisciplinary Digital Publishing Institute) doi: 10.3390/rs13050876

Mahmood, R., Pielke Sr., R. A., Hubbard, K. G., Niyogi, D., Dirmeyer, P. A., McAlpine, C., ... Fall, S. (2014). Land cover changes and their biogeophysical effects on climate. *International Journal of Climatology*, *34*(4), 929–953. Retrieved 2021-10-18, from https://onlinelibrary.wiley.com/doi/abs/10.1002/joc.3736 (_eprint: https://onlinelibrary.wiley.com/doi/pdf/10.1002/joc.3736) doi: 10.1002/joc.3736

Malbéteau, Y., Merlin, O., Molero, B., Rüdiger, C., & Bacon, S. (2016, March). DisPATCh as a tool to evaluate coarse-scale remotely sensed soil moisture using localized in situ measurements: Application to SMOS and AMSR-E data in Southeastern Australia. *International Journal of Applied Earth Observation and Geoinformation*, *45*, 221–234. Retrieved 2022-12-06, from https://www.sciencedirect.com/science/article/pii/S0303243415300386 doi: 10.1016/j.jag.2015.10.002

Maselli, F., Battista, P., Chiesi, M., Rapi, B., Angeli, L., Fibbi, L., ... Gozzini, B. (2020, December). Use of Sentinel-2 MSI data to monitor crop irrigation in Mediter-

ranean areas. *International Journal of Applied Earth Observation and Geoinformation*, *93*, 102216. Retrieved 2022-11-04, from https://www.sciencedirect.com/science/article/pii/S0303243420302531 doi: 10.1016/j.jag.2020.102216

Massari, C., Modanesi, S., Dari, J., Gruber, A., De Lannoy, G. J. M., Girotto, M., ... Brocca, L. (2021, January). A Review of Irrigation Information Retrievals from Space and Their Utility for Users. *Remote Sensing*, *13*(20), 4112. Retrieved 2021-10-20, from https://www.mdpi.com/2072-4292/13/20/4112 (Number: 20 Publisher: Multidisciplinary Digital Publishing Institute) doi: 10.3390/rs13204112

McNairn, H., & Shang, J. (2016). A Review of Multitemporal Synthetic Aperture Radar (SAR) for Crop Monitoring. In Y. Ban (Ed.), *Multitemporal Remote Sensing: Methods and Applications* (pp. 317–340). Cham: Springer International Publishing. Retrieved 2023-01-23, from https://doi.org/10.1007/978-3-319-47037-5_15 doi: 10.1007/978-3-319-47037-5_15

Merlin, O., Chehbouni, A., Walker, J. P., Panciera, R., & Kerr, Y. H. (2008, March). A Simple Method to Disaggregate Passive Microwave-Based Soil Moisture. *IEEE Transactions on Geoscience and Remote Sensing*, *46*(3), 786–796. (Conference Name: IEEE Transactions on Geoscience and Remote Sensing) doi: 10.1109/TGRS.2007.914807

Miranda, N., Meadows, P., Piantanida, R., Recchia, A., Small, D., Schubert, A., ... Vega, F. C. (2017, July). The Sentinel-1 constellation mission performance. In *2017 IEEE International Geoscience and Remote Sensing Symposium (IGARSS)* (pp. 5541–5544). (ISSN: 2153-7003) doi: 10.1109/IGARSS.2017.8128259

Modanesi, S., Massari, C., Bechtold, M., Lievens, H., Tarpanelli, A., Brocca, L., ... De Lannoy, G. J. M. (2022, September). Challenges and benefits of quantifying irrigation through the assimilation of Sentinel-1 backscatter observations into Noah-MP. *Hydrology and Earth System Sciences*, *26*(18), 4685–4706. Retrieved 2022-10-27, from https://hess.copernicus.org/articles/26/4685/2022/ (Publisher: Copernicus GmbH) doi: 10.5194/hess-26-4685-2022

Modanesi, S., Massari, C., Gruber, A., Lievens, H., Tarpanelli, A., Morbidelli, R., & De Lannoy, G. J. M. (2021, June). Optimizing a backscatter forward operator using Sentinel-1 data over irrigated land. *Hydrology and Earth System Sciences Discussions*, 1–39. Retrieved 2021-10-20, from https://hess.copernicus.org/preprints/hess-2021-273/ (Publisher: Copernicus GmbH) doi: 10.5194/hess-2021-273

Nagaraj, D., Proust, E., Todeschini, A., Rulli, M. C., & D'Odorico, P. (2021, June). A new dataset of global irrigation areas from 2001 to 2015. *Advances in Water Resources*, *152*, 103910. Retrieved 2022-11-03, from https://www.sciencedirect.com/science/article/pii/S0309170821000658 doi: 10.1016/j.advwatres.2021.103910

Nie, W., Kumar, S. V., Peters-Lidard, C. D., Zaitchik, B. F., Arsenault, K. R., Bindlish, R., & Liu, P.-W. (2022). Assimilation of Remotely Sensed Leaf Area Index Enhances the Estimation of Anthropogenic Irrigation Water Use. *Journal of Advances in Modeling Earth Systems*, *14*(11), e2022MS003040. Retrieved 2022-11-17, from https://onlinelibrary.wiley.com/doi/abs/10.1029/2022MS003040 (_eprint: https://onlinelibrary.wiley.com/doi/pdf/10.1029/2022MS003040) doi: 10.1029/2022MS003040

Niu, G.-Y., Yang, Z.-L., Mitchell, K. E., Chen, F., Ek, M. B., Barlage, M., ... Xia, Y. (2011). The community Noah land surface model with multiparameterization options (Noah-MP): 1. Model description and evaluation with local-scale measurements. *Journal of Geophysical Research: Atmospheres*, *116*(D12). Retrieved 2022-02-08, from https://onlinelibrary.wiley.com/doi/abs/10.1029/2010JD015139 (_eprint: https://onlinelibrary.wiley.com/doi/pdf/10.1029/2010JD015139) doi: 10.1029/2010JD015139

Olivera-Guerra, L., Merlin, O., & Er-Raki, S. (2020, March). Irrigation retrieval from Landsat optical/thermal data integrated into a crop water balance model: A case study over winter wheat fields in a semi-arid region. *Remote Sensing of Environment*, *239*, 111627. Retrieved 2022-11-08, from https://www.sciencedirect.com/

science/article/pii/S0034425719306479 doi: 10.1016/j.rse.2019.111627

Ouaadi, N., Jarlan, L., Khabba, S., Ezzahar, J., Le Page, M., & Merlin, O. (2021, January). Irrigation Amounts and Timing Retrieval through Data Assimilation of Surface Soil Moisture into the FAO-56 Approach in the South Mediterranean Region. *Remote Sensing*, *13*(14), 2667. Retrieved 2021-10-20, from https://www.mdpi.com/2072-4292/13/14/2667 (Number: 14 Publisher: Multidisciplinary Digital Publishing Institute) doi: 10.3390/rs13142667

Ozdogan, M., & Gutman, G. (2008, September). A new methodology to map irrigated areas using multi-temporal MODIS and ancillary data: An application example in the continental US. *Remote Sensing of Environment*, *112*(9), 3520–3537. Retrieved 2022-11-03, from https://www.sciencedirect.com/science/article/pii/S0034425708001338 doi: 10.1016/j.rse.2008.04.010

Ozdogan, M., Rodell, M., Beaudoing, H. K., & Toll, D. L. (2010, February). Simulating the Effects of Irrigation over the United States in a Land Surface Model Based on Satellite-Derived Agricultural Data. *Journal of Hydrometeorology*, *11*(1), 171–184. Retrieved 2022-11-07, from https://journals.ametsoc.org/view/journals/hydr/11/1/2009jhm1116_1.xml (Publisher: American Meteorological Society Section: Journal of Hydrometeorology) doi: 10.1175/2009JHM1116.1

Patel, P., Srivastava, H. S., Panigrahy, S., & Parihar, J. S. (2006, January). Comparative evaluation of the sensitivity of multi-polarized multi-frequency SAR backscatter to plant density. *International Journal of Remote Sensing*, *27*(2), 293–305. Retrieved 2022-12-06, from https://doi.org/10.1080/01431160500214050 (Publisher: Taylor & Francis _eprint: https://doi.org/10.1080/01431160500214050) doi: 10.1080/01431160500214050

Pervez, S., Budde, M., & Rowland, J. (2014, June). Mapping irrigated areas in Afghanistan over the past decade using MODIS NDVI. *Remote Sensing of Environment*, *149*, 155–165. Retrieved 2022-11-04, from https://www.sciencedirect.com/science/article/pii/S0034425714001461 doi: 10.1016/j.rse.2014.04.008

Rains, D., Lievens, H., De Lannoy, G. J. M., Mccabe, M. F., de Jeu, R. A. M., & Miralles, D. G. (2022). Sentinel-1 Backscatter Assimilation Using Support Vector Regression or the Water Cloud Model at European Soil Moisture Sites. *IEEE Geoscience and Remote Sensing Letters*, *19*, 1–5. (Conference Name: IEEE Geoscience and Remote Sensing Letters) doi: 10.1109/LGRS.2021.3073484

Rodríguez-Fernández, N. J., Anterrieu, E., Rougé, B., Boutin, J., Picard, G., Pellarin, T., ... Kerr, Y. H. (2019, July). SMOS-HR: A High Resolution L-Band Passive Radiometer for Earth Science and Applications. In *IGARSS 2019 - 2019 IEEE International Geoscience and Remote Sensing Symposium* (pp. 8392–8395). (ISSN: 2153-7003) doi: 10.1109/IGARSS.2019.8897815

Roebber, P. J. (2009, April). Visualizing Multiple Measures of Forecast Quality. *Weather and Forecasting*, *24*(2), 601–608. Retrieved 2022-08-25, from https://journals.ametsoc.org/view/journals/wefo/24/2/2008waf2222159_1.xml (Publisher: American Meteorological Society Section: Weather and Forecasting) doi: 10.1175/2008WAF2222159.1

Ryu, D., Crow, W. T., Zhan, X., & Jackson, T. J. (2009, June). Correcting Unintended Perturbation Biases in Hydrologic Data Assimilation. *Journal of Hydrometeorology*, *10*(3), 734–750. Retrieved 2022-11-09, from https://journals.ametsoc.org/view/journals/hydr/10/3/2008jhm1038_1.xml (Publisher: American Meteorological Society Section: Journal of Hydrometeorology) doi: 10.1175/2008JHM1038.1

Salmon, J. M., Friedl, M. A., Frolking, S., Wisser, D., & Douglas, E. M. (2015, June). Global rain-fed, irrigated, and paddy croplands: A new high resolution map derived from remote sensing, crop inventories and climate data. *International Journal of Applied Earth Observation and Geoinformation*, *38*, 321–334. Retrieved 2021-10-20, from https://www.sciencedirect.com/science/article/pii/S0303243415000240 doi: 10.1016/j.jag.2015.01.014

Siebert, S., Kummu, M., Porkka, M., Döll, P., Ramankutty, N., & Scanlon, B. R. (2015,

March). A global data set of the extent of irrigated land from 1900 to 2005. *Hydrology and Earth System Sciences*, *19*(3), 1521–1545. Retrieved 2022-10-27, from https://hess.copernicus.org/articles/19/1521/2015/ (Publisher: Copernicus GmbH) doi: 10.5194/hess-19-1521-2015

Thiery, W., Davin, E. L., Lawrence, D. M., Hirsch, A. L., Hauser, M., & Seneviratne, S. I. (2017). Present-day irrigation mitigates heat extremes. *Journal of Geophysical Research: Atmospheres*, *122*(3), 1403–1422. Retrieved 2021-10-18, from https://onlinelibrary.wiley.com/doi/abs/10.1002/2016JD025740 (_eprint: https://onlinelibrary.wiley.com/doi/pdf/10.1002/2016JD025740) doi: 10.1002/2016JD025740

Thiery, W., Visser, A. J., Fischer, E. M., Hauser, M., Hirsch, A. L., Lawrence, D. M., ... Seneviratne, S. I. (2020, January). Warming of hot extremes alleviated by expanding irrigation. *Nature Communications*, *11*(1), 290. Retrieved 2021-09-29, from https://www.nature.com/articles/s41467-019-14075-4 (Bandiera_abtest: a Cc_license_type: cc_by Cg_type: Nature Research Journals Number: 1 Primary_atype: Research Publisher: Nature Publishing Group Subject_term: Attribution;Climate and Earth system modelling;Hydrology Subject_term_id: attribution;climate-and-earth-system-modelling;hydrology) doi: 10.1038/s41467-019-14075-4

Torres, R., Snoeij, P., Geudtner, D., Bibby, D., Davidson, M., Attema, E., ... Rostan, F. (2012, May). GMES Sentinel-1 mission. *Remote Sensing of Environment*, *120*, 9–24. Retrieved 2022-11-04, from https://www.sciencedirect.com/science/article/pii/S0034425712000600 doi: 10.1016/j.rse.2011.05.028

Valmassoi, A., & Keller, J. D. (2022). A review on irrigation parameterizations in Earth system models. *Frontiers in Water*, *4*. Retrieved 2023-02-07, from https://www.frontiersin.org/articles/10.3389/frwa.2022.906664

van Eekelen, M. W., Bastiaanssen, W. G. M., Jarmain, C., Jackson, B., Ferreira, F., van der Zaag, P., ... Luxemburg, W. M. J. (2015, February). A novel approach to estimate direct and indirect water withdrawals from satellite measurements: A case study from the Incomati basin. *Agriculture, Ecosystems & Environment*, *200*, 126–142. Retrieved 2022-11-08, from https://www.sciencedirect.com/science/article/pii/S0167880914004861 doi: 10.1016/j.agee.2014.10.023

van Leeuwen, P. J. (2015). Representation errors and retrievals in linear and nonlinear data assimilation. *Quarterly Journal of the Royal Meteorological Society*, *141*(690), 1612–1623. Retrieved 2023-01-26, from https://onlinelibrary.wiley.com/doi/abs/10.1002/qj.2464 (_eprint: https://onlinelibrary.wiley.com/doi/pdf/10.1002/qj.2464) doi: 10.1002/qj.2464

Vogels, M. F. A., de Jong, S. M., Sterk, G., Wanders, N., Bierkens, M. F. P., & Addink, E. A. (2020, June). An object-based image analysis approach to assess irrigation-water consumption from MODIS products in Ethiopia. *International Journal of Applied Earth Observation and Geoinformation*, *88*, 102067. Retrieved 2022-11-04, from https://www.sciencedirect.com/science/article/pii/S0303243419311833 doi: 10.1016/j.jag.2020.102067

Vreugdenhil, M., Wagner, W., Bauer-Marschallinger, B., Pfeil, I., Teubner, I., Rüdiger, C., & Strauss, P. (2018, September). Sensitivity of Sentinel-1 Backscatter to Vegetation Dynamics: An Austrian Case Study. *Remote Sensing*, *10*(9), 1396. Retrieved 2022-12-06, from https://www.mdpi.com/2072-4292/10/9/1396 (Number: 9 Publisher: Multidisciplinary Digital Publishing Institute) doi: 10.3390/rs10091396

Xie, Y., & Lark, T. J. (2021, July). Mapping annual irrigation from Landsat imagery and environmental variables across the conterminous United States. *Remote Sensing of Environment*, *260*, 112445. Retrieved 2022-11-04, from https://www.sciencedirect.com/science/article/pii/S0034425721001632 doi: 10.1016/j.rse.2021.112445

Zappa, L., Schlaffer, S., Bauer-Marschallinger, B., Nendel, C., Zimmerman, B., & Dorigo, W. (2021, January). Detection and Quantification of Irrigation Water Amounts at 500 m Using Sentinel-1 Surface Soil Moisture. *Remote Sensing*, *13*(9), 1727. Retrieved 2021-10-20, from https://www.mdpi.com/2072-4292/13/9/1727 (Number:

9 Publisher: Multidisciplinary Digital Publishing Institute) doi: 10.3390/rs13091727

Zappa, L., Schlaffer, S., Brocca, L., Vreugdenhil, M., Nendel, C., & Dorigo, W. (2022, September). How accurately can we retrieve irrigation timing and water amounts from (satellite) soil moisture? *International Journal of Applied Earth Observation and Geoinformation*, *113*, 102979. Retrieved 2022-08-24, from https://www.sciencedirect.com/science/article/pii/S1569843222001704 doi: 10.1016/j.jag.2022.102979

Zaussinger, F., Dorigo, W., Gruber, A., Tarpanelli, A., Filippucci, P., & Brocca, L. (2019, February). Estimating irrigation water use over the contiguous United States by combining satellite and reanalysis soil moisture data. *Hydrology and Earth System Sciences*, *23*(2), 897–923. Retrieved 2022-11-07, from https://hess.copernicus.org/articles/23/897/2019/ (Publisher: Copernicus GmbH) doi: 10.5194/hess-23-897-2019

Zhang, C., Dong, J., & Ge, Q. (2022, October). IrriMap_cn: Annual irrigation maps across China in 2000–2019 based on satellite observations, environmental variables, and machine learning. *Remote Sensing of Environment*, *280*, 113184. Retrieved 2022-08-02, from https://www.sciencedirect.com/science/article/pii/S0034425722002966 doi: 10.1016/j.rse.2022.113184

Zhang, L., Zhang, K., Zhu, X., Chen, H., & Wang, W. (2022, October). Integrating remote sensing, irrigation suitability and statistical data for irrigated cropland mapping over mainland China. *Journal of Hydrology*, *613*, 128413. Retrieved 2022-11-04, from https://www.sciencedirect.com/science/article/pii/S0022169422009830 doi: 10.1016/j.jhydrol.2022.128413

Zohaib, M., & Choi, M. (2020, April). Satellite-based global-scale irrigation water use and its contemporary trends. *Science of The Total Environment*, *714*, 136719. Retrieved 2022-11-07, from https://www.sciencedirect.com/science/article/pii/S0048969720302291 doi: 10.1016/j.scitotenv.2020.136719

**Figure 1.**

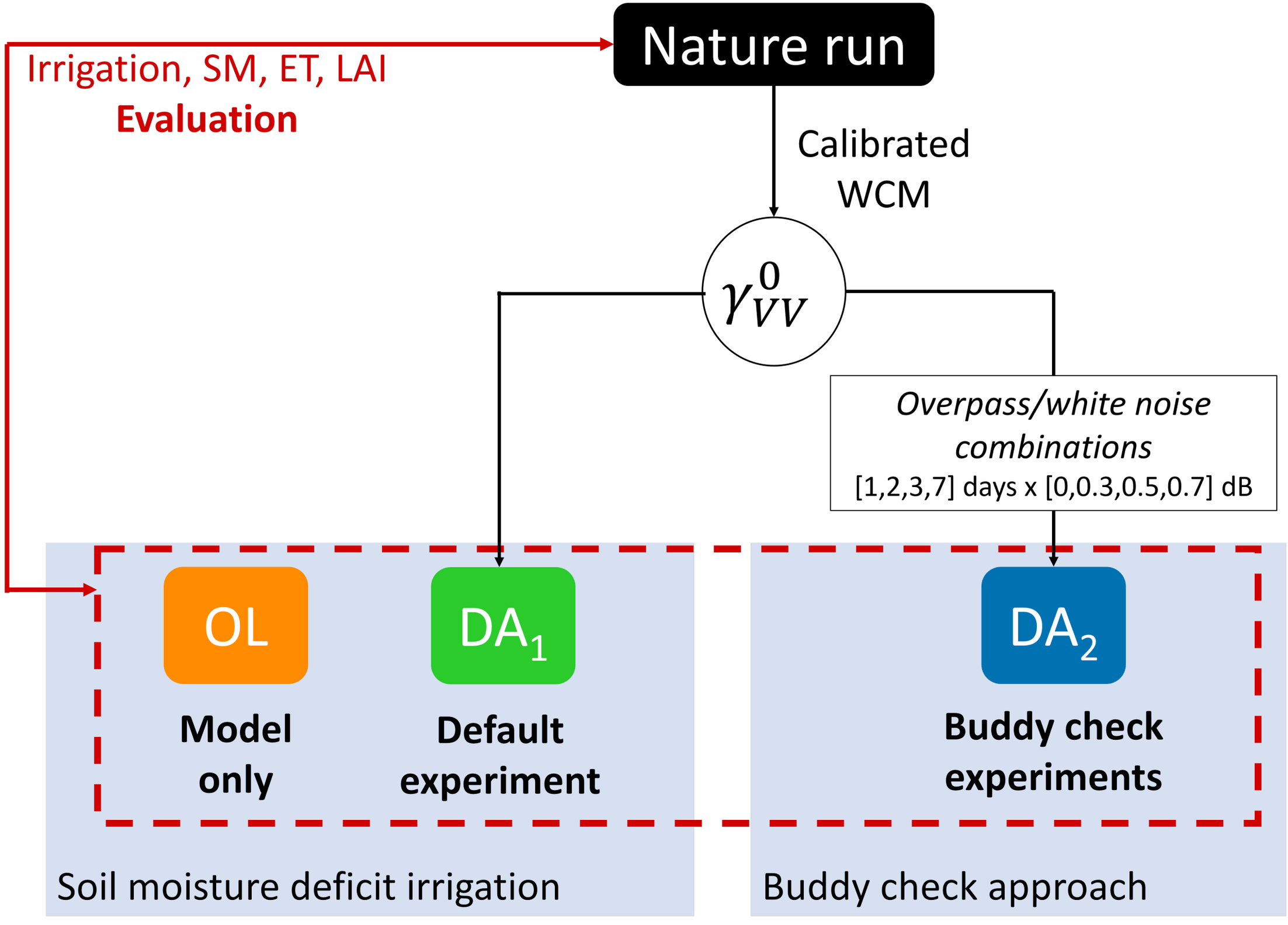
Nature run
Irrigation, SM, ET, LAI
Evaluation
Calibrated
WCM
$\gamma^0_{VV}$
*Overpass/white noise combinations*
[1,2,3,7] days x [0,0.3,0.5,0.7] dB
OL
$DA_1$
$DA_2$
**Model only**
**Default experiment**
**Buddy check experiments**
Soil moisture deficit irrigation
Buddy check approach

**Figure 2.**

(a)

(b)

(c)

innov [dB]

Δinnov [dB]

MA [-]

irrigation [mm day$^{-1}$]

5
0
−5

0.6
0.4

300
200
100
0

2012-05-01
2012-06-01
2012-07-01
2012-08-01
2012-09-01

nature
$DA_{2,H}$
$2.5 * SD_{innov,20}$

**Figure 3.**

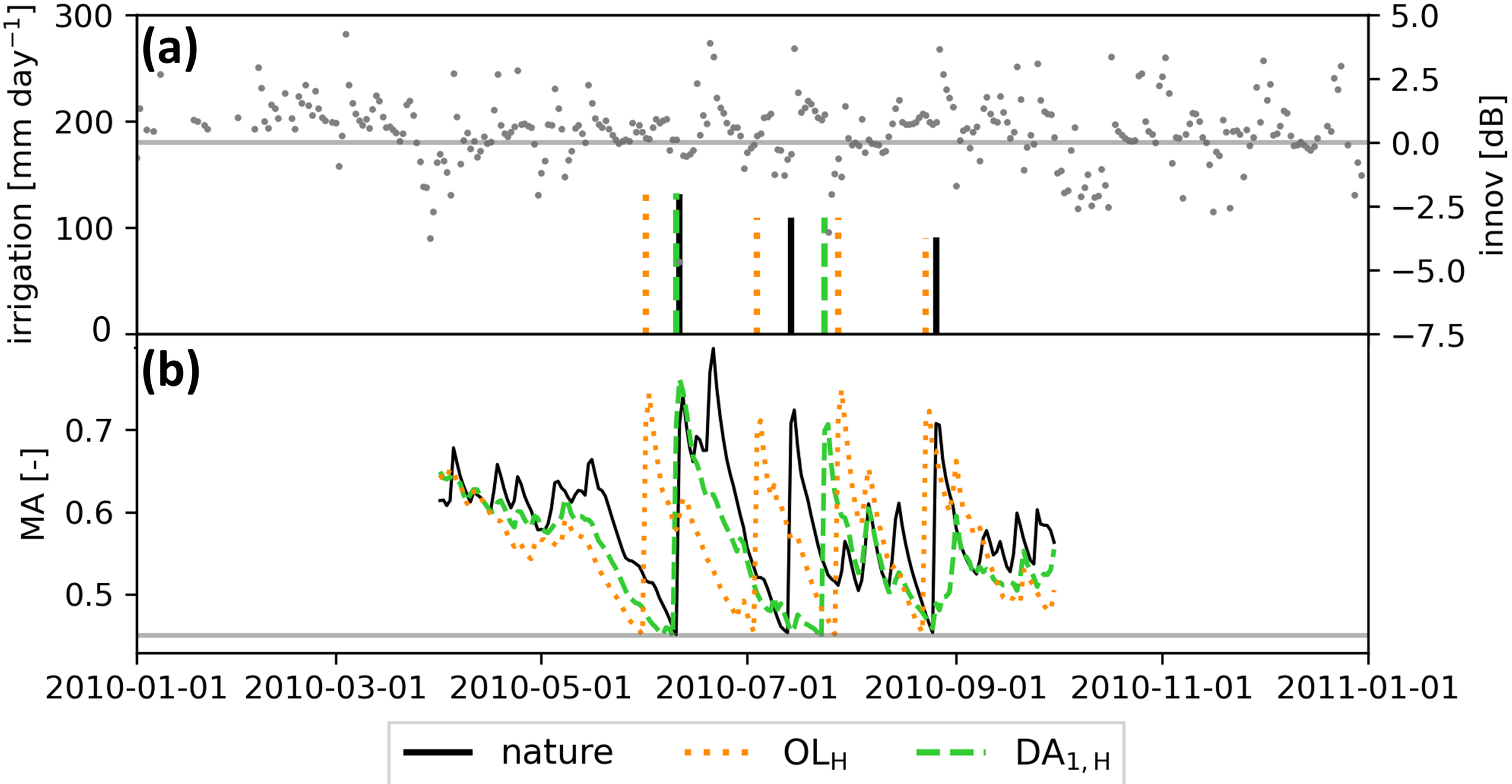
(a)
(b)
irrigation [mm day$^{-1}$]
innov [dB]
MA [-]
300
200
100
0
5.0
2.5
0.0
−2.5
−5.0
−7.5
0.7
0.6
0.5
2010-01-01
2010-03-01
2010-05-01
2010-07-01
2010-09-01
2010-11-01
2011-01-01
nature
OL$_H$
DA$_{1,H}$

**Figure 4.**

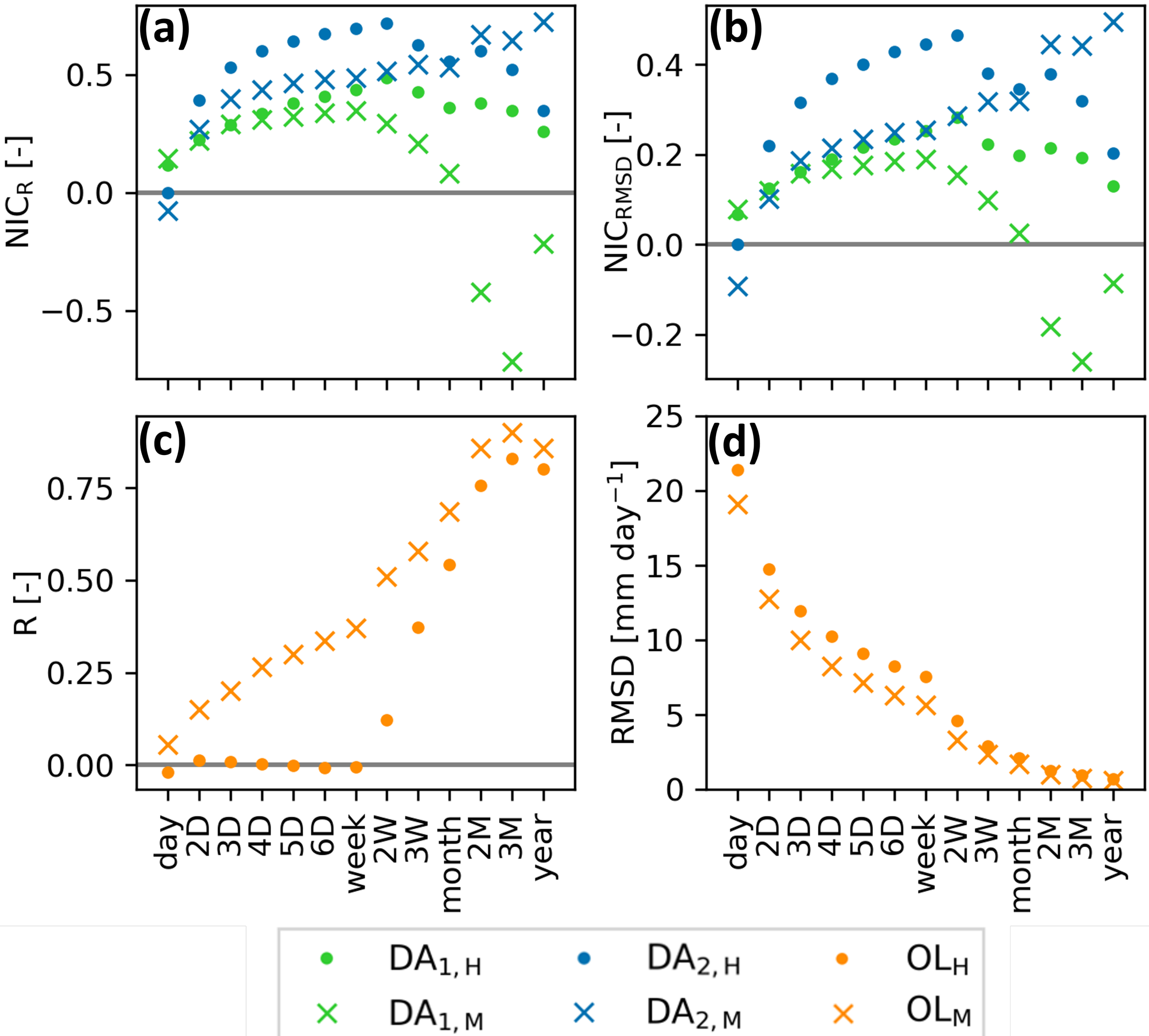
(a)
$NIC_R$ [-]
0.5
0.0
−0.5
(b)
$NIC_{RMSD}$ [-]
0.4
0.2
0.0
−0.2
(c)
R [-]
0.75
0.50
0.25
0.00
(d)
RMSD [mm day$^{-1}$]
25
20
15
10
5
0
day
2D
3D
4D
5D
6D
week
2W
3W
month
2M
3M
year
$DA_{1,H}$
$DA_{2,H}$
$OL_H$
$DA_{1,M}$
$DA_{2,M}$
$OL_M$

**Figure 5.**

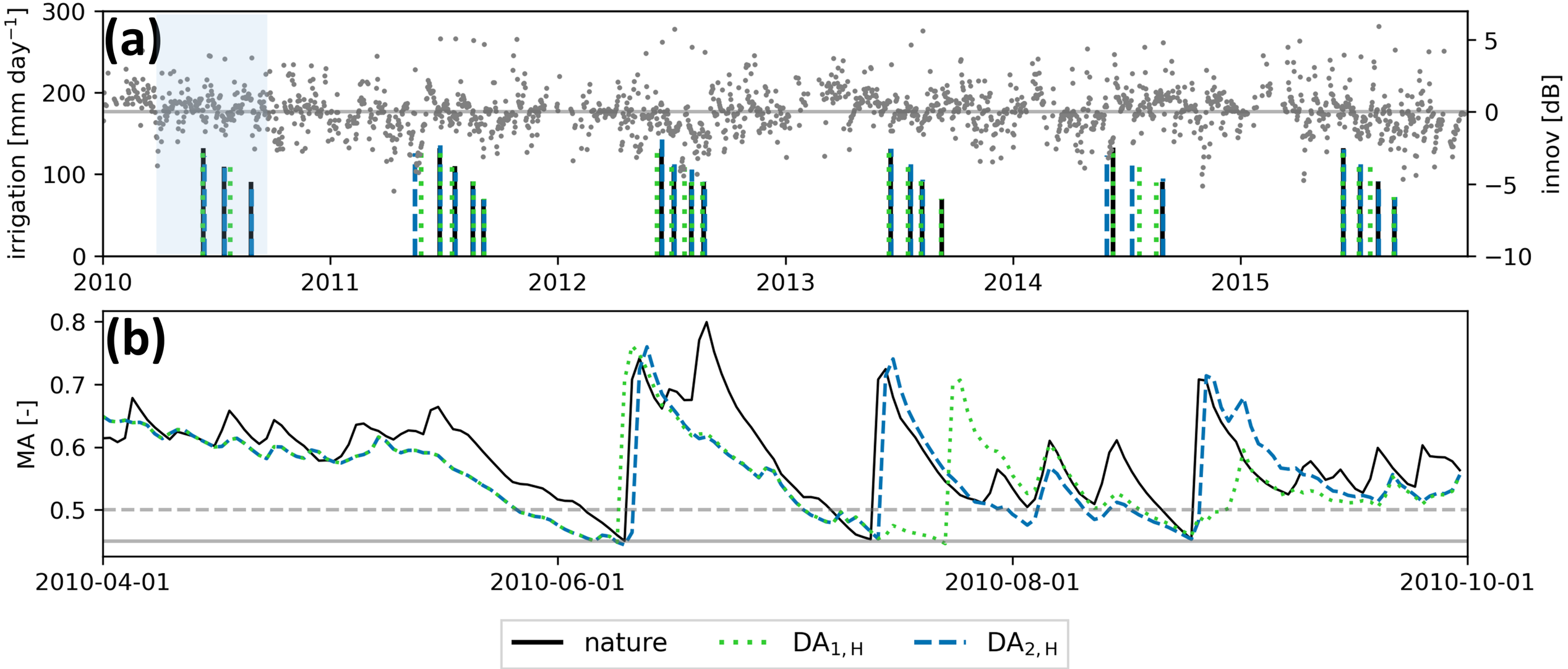
(a)
irrigation [mm day$^{-1}$]
innov [dB]
300
200
100
0
5
0
−5
−10
2010
2011
2012
2013
2014
2015
(b)
MA [-]
0.8
0.7
0.6
0.5
2010-04-01
2010-06-01
2010-08-01
2010-10-01
nature
DA$_{1,H}$
DA$_{2,H}$

**Figure 6.**

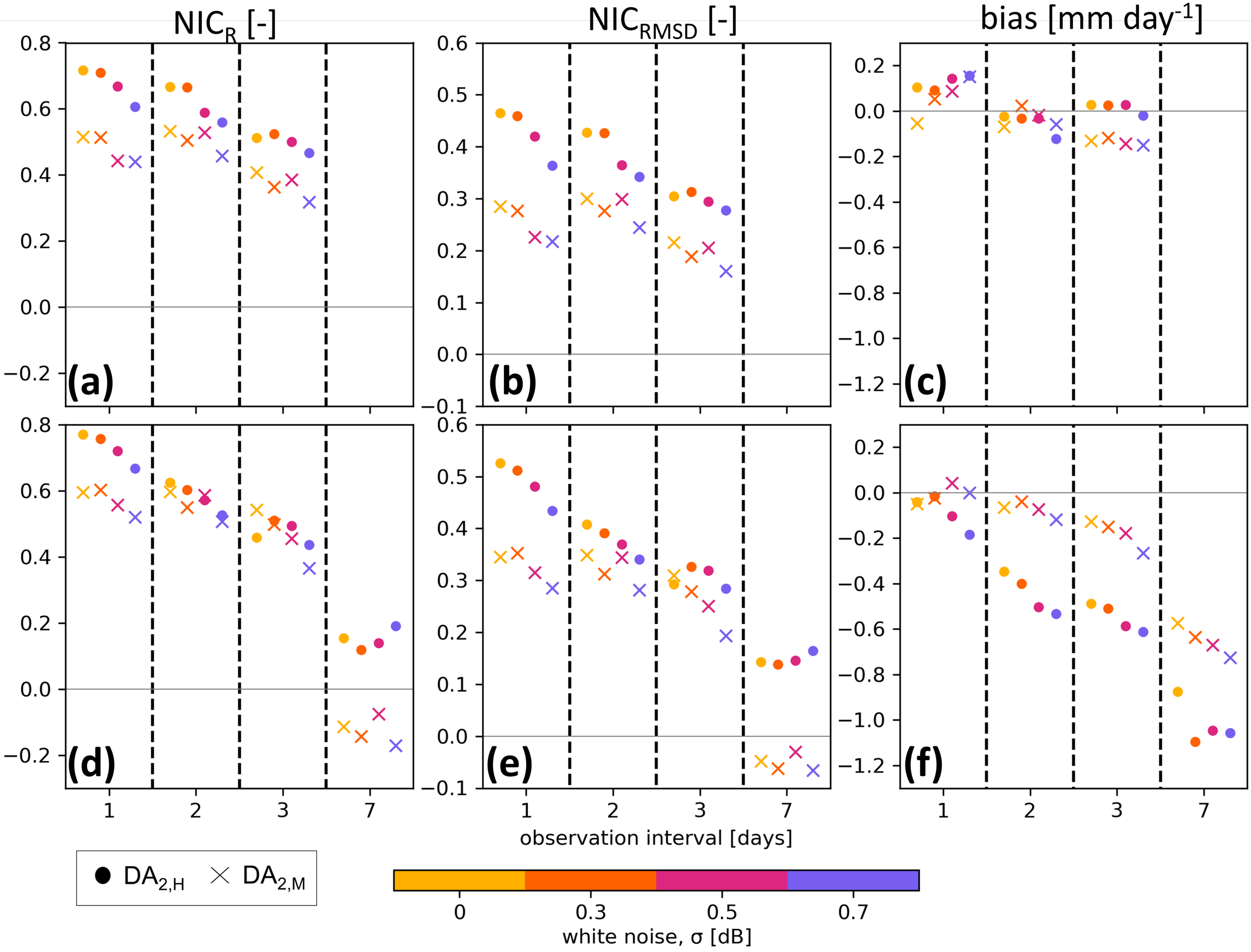
NIC$_R$ [-]
NIC$_{RMSD}$ [-]
bias [mm day$^{-1}$]
(a)
(b)
(c)
(d)
(e)
(f)
observation interval [days]
DA$_{2,H}$
DA$_{2,M}$
white noise, σ [dB]